SEISMIC PERFORMANCE ASSESSMENT OF A COLD-FORMED STEEL BUILDING

by

Emrah KURT

B.S., Civil Engineering, Kocaeli University, 2013

Submitted to the Institute for Graduate Studies in
Science and Engineering in partial fulfillment of
the requirements for the degree of
Master of Science

Graduate Program in Civil Engineering

Boğaziçi University

2019

SEISMIC PERFORMANCE ASSESSMENT OF A COLD-FORMED STEEL BUILDING

APPROVED BY:

Assoc. Prof. Serdar Soyöz (Thesis Supervisor)	.....
Assoc. Prof. Barlas Özden Çağlayan	.....
Assoc. Prof. Serdar Selamet	.....

DATE OF APPROVAL: 26.09.2019

ACKNOWLEDGEMENTS

Firstly, I would like to show best of my gratitude to my advisor and thesis supervisor, Assoc. Prof. Serdar Soyoz for his incredible help and support through this study and research. He has always been very supportive for my success. His interest and patience helped me progress in my studies and thesis.

In addition, I would like to present my gratefulness to Assoc. Prof. Serdar Selamet and Assoc. Prof. Barlas Özden Çağlayan for their great and supportive attitude towards me, and for their valuable recommendations.

I owe special appreciation to Özlem Altıkulaç who has never stopped motivating and supporting me during my study just like she does for all the parts she takes place in my life.

I would like to express my sincere gratitude to Ömer Çitil and Erdem Koç for their great support.

I would also like to show my appreciation to my firends, Cem Şentürk, Ramazan Sözer, Volkan Koçbay and Necati Murat Dinçtürk for their great support and joy of living.

Lastly, I wish to thank the beloved members of my family. They have always unconditionally supported me throughout my life.

ABSTRACT

SEISMIC PERFORMANCE ASSESSMENT OF A COLD-FORMED STEEL BUILDING

In the scope of this thesis, lateral load bearing capacity of cold formed steel shear panel is investigated experimentally and analytically. In residential construction applications, cold formed steel frame is covered with various sheathings depending on its architectural and design purpose. The lateral load bearing capacity of the structure depends on sheathing type, screw spacing, screw type, cold formed steel element thickness, anchor type, anchor spacing and aspect ratio. Light steel structures, which are becoming more common day by day, force the countries to establish their own design standards. In this context, experiments have been carried out in Boğaziçi University Structural Laboratory to be used in the new earthquake specification. Force deformation relation were obtained in these experiments which were including different screw spacing and different steel thicknesses.

This thesis aims to find a simple solution by eliminating this complexity. Based on the experimental results, an equivalent diagonal strut model was proposed to represent the effect of sheathing. This method, which was previously used in the modeling of reinforced concrete walls of RC building was used here for cold-formed steel panels. For equivalent diagonal strut, the thickness is important to represent lateral stiffness of the panel, and this thickness is proposed with an equation.However, this equation has only been proposed for this study, and the formula needs to be studied and developed in future studies. These panels were analyzed in SAP2000 program and it was observed that the results were convergent with the experimental results. This formula aims to provide ease of calculation by putting aside the complexity of explicit screws modeling modeling of sheathing between sheathing and steel.

Performance analysis of a CFS building under seismic loading was conducted. It was also concluded that such structures were safe to be built in earthquake prone countries.

ÖZET

TEK KATLI HAFİF ÇELİK BİR YAPININ DEPREM PERFORMANS DEĞERLENDİRMESİ

Bu tezin kapsamında, hafif çelik çerçeveli kayma panellerin yanal yük taşıma kapasitesi deneysel ve analitik olarak incelenmiştir. Konut yapımı uygulamalarında hafif çelik çerçeve, mimari ve tasarım amacına bağlı olarak çeşitli kaplamalar ile kaplanır. Yapının yanal yük taşıma kapasitesi kaplama tipi, vida aralığı, vida çeşidi, hafif çeliğin kalınlığı, ankraj tipi, ankraj aralığına ve en boy oranına bağlıdır. Her geçen gün yaygınlaşan hafif çelik yapılar ülkelerin kendi tasarım standartlarını oluşturmaya zorlamaktadır. Bu bağlamda yeni deprem yönetmeliğinde kullanılması amacıyla Boğaziçi Üniversitesi Yapı Laboratuvarında bu deneyler yapılmıştır. Deneylere farklı vida aralıkları ve farklı çelik kalınlıkları dahil edilerek yük şekil değiştirme ilişkisi elde edilmiştir.

Bu tezde bu karmaşıklık ortadan kaldırılarak basit bir çözüm yolu bulmak amaçlanmıştır. Deney sonuçları göz önünde bulundurularak çıkılarak bu panellerin etkisini temsilen yeni bir eşdeğer çapraz çubuk modeli önerilmiştir. Önceleri betonarme duvarların matematiksel olarak modellenmesinde kullanılan bu yöntem bu çalışmada hafif çelik paneller için uygulanmıştır. Eşdeğer çapraz dikmenin kalınlığı yatay rijitliği temsil ettiği için önemlidir ve bu kalınlık bir eşitlikle önerilmiştir. Fakat bu eşitlik sadece bu çalışma için önerilmiştir ve kesinlikle gelecekteki çalışmalarda üzerinde çalışılıp geliştirilmelidir. Bu paneller SAP2000 programı yardımıyla matematiksel olarak elde edilmiştir ve bu çalışmada deney sonuçlarıyla yakınsak sonuçlar elde edilmiştir. Bu formül vida elemanlarının kullanıldığı panellerdeki karmaşıklığı bir kenara koyarak hesap kolaylığı sağlamayı amaçlamaktadır.

Hafif çelik yapının deprem yükleri altında performans analizi yapılmıştır. Ayrıca depreme yatkın olan ülkelerde hafif çelik yapıların inşa edilmesinin güvenli olduğu

sonucu çıkarılmıştır.

TABLE OF CONTENTS

ACKNOWLEDGEMENTS . . . iii
ABSTRACT . . . iv
ÖZET . . . vi
LIST OF FIGURES . . . xi
LIST OF TABLES . . . xv
LIST OF SYMBOLS . . . xvi
LIST OF ACRONYMS/ABBREVIATIONS . . . xxi
1. INTRODUCTION . . . 1
1.1. General . . . 1
1.2. An Introduction to Cold-Formed Steel Structures . . . 3
1.2.1. Production of Cold-Formed Steel Profiles . . . 3
1.2.2. Construction Methods of CFS buildings . . . 4
1.2.2.1. Frame System . . . 4
1.2.2.2. Panel System . . . 5
1.2.2.3. Modular System . . . 5
1.2.3. Load Carrying Methodology of CFS Structures . . . 6
1.3. Literature Review . . . 8
1.3.1. Existing Codes, Standards and Software . . . 8
1.3.2. Literature Review . . . 9
1.4. Scope and Motivation of the Thesis . . . 25
1.5. Thesis Overview . . . 27
2. EXPERIMENTAL STUDY ON VARIOUS CFS SHEAR PANELS . . . 28
2.1. Introduction . . . 28
2.2. Configuration of Shear Panel . . . 28
2.3. List of Shear Panels . . . 28
2.4. Loading Protocol and Loading Frame . . . 30
2.5. Test Results . . . 33
2.5.1. Test result of the Panel with 0.9 mm steel thickness and 100-150 mm screw spacing . . . 33

2.5.2. Test result of the Panel with 0.9 mm steel thickness and 200 mm screw spacing . . . 34
2.5.3. Test Result of the Panel with 1.5 mm steel thickness and 200 mm spacing . . . 35
2.6. Photos of the Experiment . . . 36
3. ANALYTICAL STUDY ON EXPERIMENTAL VALUES . . . 39
3.1. Introduction . . . 39
3.2. The Basis of the Analytical Approach . . . 41
3.3. Stiffness Determination of the CFS Panel Due to Experimental Results 47
3.3.1. The Panel with 100 and 150 mm screw spacing and 0.9 mm steel thickness . . . 48
3.3.2. The Panel with 200 mm screw spacing and 0.9 mm steel thickness 49
3.3.3. The Panel with 200 mm screw spacing and 1.5 mm steel thickness 50
3.4. Analytical Investigation of the Panel Stiffness . . . 51
3.4.1. The Panel with 100/300 screw spacing and 0.9 mm steel thickness 52
3.4.2. The Panel with 150/300 screw spacing and 0.9 mm steel thickness 54
3.4.3. The Panel with 200/300 screw spacing and 0.9 mm steel thickness 56
3.4.4. The Panel with 200/300 screw spacing and 1.5 mm steel thickness 57
3.5. Comparision of the Experimental and Analytical Results in terms of Lateral Stiffness . . . 59
3.6. The Equivalent Strut Width Proposal . . . 59
4. ANALYTICAL STUDY OF A TYPICAL ONE-STORY CFS STRUCTURE CREATED WITH DIAGONAL STRUTS . . . 61
4.1. Introduction . . . 61
4.2. Properties of the Structure . . . 61
4.3. Loads Assigned to the Structure . . . 63
4.3.1. Dead, Live and Snow Loads . . . 63
4.3.2. Earthquake Loads . . . 63
4.4. Load Combinations . . . 67
4.5. Demands of the Structure . . . 67
4.5.1. Shear Demand . . . 67

4.5.2. Axial Demand 68
4.6. Capacity Calculations 69
4.6.1. Section Properties 69
4.6.2. Nominal Buckling Stress for Column Buckling of Stud between Fasteners (Elastic Flexural Buckling) 70
4.6.3. Elastic Torsional Buckling 72
4.6.4. Nominal Buckling Stress for Overall Column Buckling 73
4.6.5. Torsional-Flexural Overall Column Buckling 75
4.6.6. Local Buckling 76
4.6.7. Distortional Buckling 77
4.6.8. Axial Capacity 78
4.6.9. Shear Capacity 79
5. CONCLUSIONS AND FUTURE WORKS 80
5.1. List of Conclusions 80
5.2. Future Works 81
REFERENCES 82

LIST OF FIGURES

Figure 1.1. Cold-Formed Steel Building Under Construction [1] 2

Figure 1.2. Completed Cold-Formed Steel Building [2] 2

Figure 1.3. Some widespread cold-formed steel profiles [1] 3

Figure 1.4. Rolling Machine [1] 4

Figure 1.5. Frame System [1] 4

Figure 1.6. Constructon of a CFS building by Panel System [1] 5

Figure 1.7. A CFS structure made with modular system [3] 6

Figure 1.8. Details of a CFS panel (Fiorino *et al.*) 7

Figure 1.9. Cold-formed steel with sheathing panel detail [1] 8

Figure 1.10. Configuration of Type A,B and C Walls 10

Figure 1.11. 3D view of test prototype 13

Figure 1.12. LD Nomographs 15

Figure 1.13. NS Nomographs 16

Figure 1.14. OC Nomographs 18

Figure 1.15. Deformation Component of a Sheathed CFS Shear Wall 19

Figure 1.16. An infilled frame under lateral load: (a) actual system, (b) macro-model 21

Figure 1.17. Components of a typical CFS shear panel 23

Figure 1.18. CFS panel and its analytical model of a CFS panel 25

Figure 2.1. Cross sections of cold formed steel members 29

Figure 2.2. Configuration of shear panel 29

Figure 2.3. Hyraulic Actuator and Reaction Frame 30

Figure 2.4. Test Steps and Number of Cycle 32

Figure 2.5. Experimental results of the Panel with 100 and 150 mm screw spacing 33

Figure 2.6. Experimental results of the Panel with 200 mm screw spacing . . . 34

Figure 2.7. Experimental Results of the Panel with 200 mm and 1.5 mm steel thickness 35

Figure 2.8. Deformed CFS panel after loading 36

Figure 2.9. Damage observed at peak displacement of 50 mm 37

Figure 2.10. Damage observed at peak displacement of 100 mm 38

Figure 3.1. A completed analytical model of the CFS panel 39

Figure 3.2. An extruded view of the analytical diagonal strut model 40

Figure 3.3. A typical sketch of the analytical strut model 41

Figure 3.4. Deformed shape of the unit 42

Figure 3.5. Deformation under top load 43

Figure 3.6. Deformation under bottom load 44

Figure 3.7. Experimental results of the Panel with 100 and 150 mm screw spacing 48

Figure 3.8. Experimental results of the Panel with 200 mm screw spacing . . 49

Figure 3.9. Experimental result of the Panel with steel thickness 1.5 mm and 200 mm screw spacing 50

Figure 3.10. Analytical model of the strut model 51

Figure 3.11. Lateral load and displacement values 52

Figure 3.12. Lateral load and displacement values 54

Figure 3.13. Experimental results of the Panel with 200 mm screw spacing . . 56

Figure 3.14. Lateral load and displacement values 57

Figure 4.1. Plan view of the structure 61

Figure 4.2. Extruded-3D View of the Structure 62

Figure 4.3. Maximum Axial Force (kN) 68

Figure 4.4. Dimensions of the double C cross section 69

Figure 4.5. Sheathing Parameters 74

LIST OF TABLES

Table 1.1. List of CFS shear panels 24

Table 2.1. Shear Panel Specimens 30

Table 2.2. Test Steps and Number of Cycles 31

Table 3.1. Cross Section Properties of the CFS Panel 47

Table 3.2. Comparision of the experimental and analytical results 59

Table 4.1. Mechanical properties of gypsum wallboard and CFS 62

Table 4.2. Weight of the structure 63

Table 4.3. Earthquake Parameters 64

Table 4.4. Total base shear force 66

Table 4.5. Maximum Axial Force 68

Table 4.6. Section Properties 70

LIST OF SYMBOLS

a	Shear anchor spacing
A	Gross cross-sectional area of an end stud
A_b	Area of the beam section
A_c	Area of the double stud section
A_e	Effective area
A_g	Gross area
c	Spacing of the studs
C_oG_y	Center of gravity about y
C_w	Warping constant of torsion of cross section
d	Generic displacement
d_a	Overturning deformation
d_b	Bending deformation
d_f	Sheathing fasteners deformation
d_s	Sheathing panels shear deformation
d_u	Ultimate displacement
d_Y	Yield displacement
d_C	Seismic displacement capacity
d_D	Seismic displacement demand
D_d	Lateral stiffness of sheathing
D_i	Lateral stiffness of the simplified model
D_f	Lateral stiffness of bare frame
D_{max}	Referance deformation
e	Edge distance
E	Modulus of elasticity of the panel material
E_b	Modulus of elasticity of beam material
E_c	Modulus of elasticity of column material
E_d	Modulus of elasticity of panel
E_{dx}	Earthquake load in x direction

E_{dy}	Earthquake load in y direction
E_{dz}	Vertical earthquake load
f_H	Function representing wall shear strength
f_K	Function representing wall shear stiffness
f_{sad}	Function of spectral acceleration
f_y	Function representing wall yield displacement
f_Y	Nominal yield strength
F_1	Local ground coefficients
F_e	Elastic buckling stress
F_n	Nominal buckling stress
F_{cs}	Compressive force on the diagonal strut
F_{db}	Distortinal buckling stress
F_{tlc}	The tensile force on the left column
F_{tub}	The tensile force on the upper track
F_u	ultimate load
F_y	Yield stress
G	Shear modulus of elasticity of the panel material
g	Gravitational acceleration
h	Height of panel
h_v	Height of the opening
H_c	Seismic strength capacity
H_D	Seismic action demand
$\bar{H}_c$	Wall shear strength per wall unit length
$\bar{H}_{c,f}$	Resistance of sheathing fasteners
$\bar{H}_{c,s}$	Resistance of studs
$\bar{H}_{c,ha}$	Resistance of hold-down anchors
$\bar{H}_{c,sa}$	Resistance of shear anchors
$\bar{H}_{c,s,k}$	Shear characteristic strength of studs per wall unit length
$\bar{H}_{c,ha,k}$	Shear characteristic strength of hold-down anchors per wall unit length
$\bar{H}_{c,sa,k}$	Shear characteristic strength of shear anchors per wall unit length

$\bar{H}_{c,f,d}$	Shear design strength of sheathing fasteners per wall unit length
I	Importance factor
I_b	Moment of inertia of beam
I_c	Moment of inertia of column
J	St. Venant torsion constant of cross section
k_b	Axial stiffness of the track
k_c	Axial stiffness of the stud
k_d	Axial stiffness of the panel
$k_{\phi fe}$	Elastic rotational spring stiffness of the flange
$k_{\phi fg}$	Geometric rotational stiffness of the flange
$k_{\phi we}$	Elastic stiffness of the web
$k_{\phi wg}$	Rotational stiffness of the web
K_a	Axial stiffness of the hold-down device
K_e	Elastic stiffness
l	Length of the panel
l_v	Length of the opening
l'	Length of the beam
N_{ha}	Tension axial strength of hold-down anchor
N_s	The stud compression axial strength
p	Interior spacing
P_n	Axial load
P_{peak}	Lateral Peak Load
P_u	Ultimate axial load
P_{yield}	Yield force
Q	Required allowable shear strength of connection
$\bar{Q}$	Design shear rigidity for two wallboards
$\bar{Q}_0$	Sheathing parameter
r_0	Polar radius of gyration of cross section about shear center
r_x	Radius of gyration of cross section about centroidal principal axis

r_y	Radius of gyration of cross section about centroidal principal axis
s	Sheathing-to-frame fastener exterior spacing
S_1	The map spectral acceleration coefficient for the 1.0 second period
S_a	Spectral acceleration
$S_{ae}(T)$	Horizontal elastic spectral acceleration
$S_{aeD}(T)$	Vertical elastic spectral acceleration
S_{D1}	Design spectral acceleration coefficient
S_{DS}	Design spectral acceleration coefficient
S_s	Description of
t_s	Thickness of the panel stud
t_w	Thickness of the panel sheathing
T_A,T_B	Spectrum characteristic periods
T	Period of vibration
U	Ultimate limit point
v_c	Shear strength of the panel per meter
V_c	Shear strength of the panel
V_{peak}	Shear strength
V_{sa}	Shear strength of the shear anchor
$V_{tE}^{(x)}$	Total bas shear force along x direction
w	Equivalent Strut width
W	Weight of the structure
x_0	Distance from shear center to centroid along principal x axis
y_0	Distance from shear center to centroid along principal y axis
Y	Yield limit point
$\gamma_{ov,ha}$	Overstrength factor of hold-down anchors
$\gamma_{ou,s}$	Overstrength factor of studs
$\gamma_{ou,sa}$	Overstrength factor of shear anchors
γ_f	the coefficient of susceptibility to fault
δ_{p1p2}	Mid-span displacement of the panel

δ_x	Vertical generic displacement
δ_y	Vertical generic displacement
Δ_x	Horizontal displacement
θ	Angle between the equivalent strut and horizontal axis
λ_c	Column slenderness parameter
ξ	Viscous damping ratio
σ_{CR}	Theoretical elastic buckling stress
σ_{crl}	Critical local buckling stress
σ_t	Torsional buckling stress
ϕ_c	resistance factor

LIST OF ACRONYMS/ABBREVIATIONS

3D	Three Dimensional
AISI	American Iron and Steel Institute
ASTM	American Society for Testing and Materials
CFS	Cold-Formed Steel
CUREE	Consortium of Universities for Research in Earthquake Enginnering
FE	Finite Element
FEM	Finite Element Method
GWB	Gypsum Wallboard
LD	Linear Dynamic
NBCC	National Building Code of Canada
NS	Nonlinear Static
OSB	Oriented Strand Board
SAP	Structural Analysis Program
SWP	Shear Wall Panels
TEC	Turkish Eartquake Code
TS	Turkish Standards

1. INTRODUCTION

1.1. General

Cold-formed steel (CFS) structures have been used in the United States since World War ll. Overtime, it has been adopted in many countries and its usage is increasing day by day. Cold-formed steel structures previously constructed up to one or two stories are new constructed up to four stories. Cold-formed steel structures are constructed from elements formed by shaping cold-formed sheet metal plates on rolling machines. It is especially preferred due to following properties:

- Low-weight,
- High strength / stiffness ratio,
- Ease of constructing,
- Low-cost,
- Less construction time,
- Recyclable material,

Thanks to such features, cold-formed steel (CFS) structures can be utilized for hospitals, schools, charity buildings which should be constructed immediately after natural disasters. Also, farmhouses can be easily constructed by CFS.

CFS is highly suitable for structures such as CFS – RC or CFS – wooden frame. Furthermore, damaged structural elements can be easily replaced after a challenging event.



Figure 1.1. Cold-Formed Steel Building Under Construction [1]



Figure 1.2. Completed Cold-Formed Steel Building [2]

1.2. An Introduction to Cold-Formed Steel Structures

First of all, these three remarks should be defined to understand cold-formed steel (CFS) structures such as how it is obtained, how it is applied and then how it carries the load.

1.2.1. Production of Cold-Formed Steel Profiles

Cold-formed steel members are produced according to ASTM C645 and ASTM C955 specifications. These specifications determine the dimensions of steel profiles and specify the material requirements of the bearing and non-bearing members. The material coating requirements are specified in ASTM A653/A653M and ASTM A792/A792M.

Cold-formed steel structural members are produced from steel sheet material by rolling. Some types of CFS profiles are as follows:

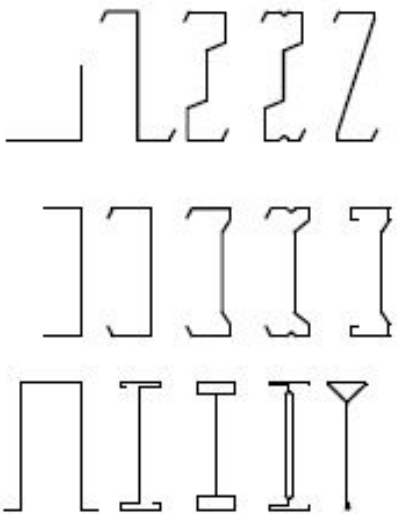

Figure 1.3. Some widespread cold-formed steel profiles [1]

CFS profiles are formed by computer-aided rolling machine.



Figure 1.4. Rolling Machine [1]

1.2.2. Construction Methods of CFS buildings

There are 3 types of construction methods that are common in the world market.

1.2.2.1. Frame System. Frame system is constructed by assembling each individual element in the field and usually used to avoid crane costs. Installation takes longer than other methods.



Figure 1.5. Frame System [1]

1.2.2.2. Panel System. Panels are formed by cold-formed steel members and sheathing materials at workshop. It is a system constructed by assembling the panels in place after transporting to the construction site.



Figure 1.6. Constructon of a CFS building by Panel System [1]

1.2.2.3. Modular System. In this type of system, it can be constructed as a part of building by combining panel system and frame system. These modules are transported from the workshop to the field and assembled other modules to obtain the building.



Figure 1.7. A CFS structure made with modular system [3]

1.2.3. Load Carrying Methodology of CFS Structures

CFS structures consist of roofs, purlins, covers, beams, columns, walls and foundations similar to conventional reinforcement concrete structures. As in typical structures, loads are transferred from slabs to beams, from beams to columns and from there to foundation, respectively. Due to vital importance of load transferring, each structural member must have correct connection. Column-beam joints in cold-formed steel structures at least in the scope of this thesis are usually pinned connection, so lateral load capacity is gained by X bracing or K bracing and sheathings. Since the panels are the subject of this thesis, it is especially necessary to examine them closely. Cold-formed steel with panel detail is given in Figure 1.8.

This panel consists of sheathing, top-bottom tracks, vertical studs, screws, hold-down anchors, shear anchors and hold-down devices. OSB (Oriented Strand Board), plywood, steel sheet or GWB (gypsum wall board) like in this study can be used as sheathing. Lateral stiffness may vary depending on sheathing type and sheathing to

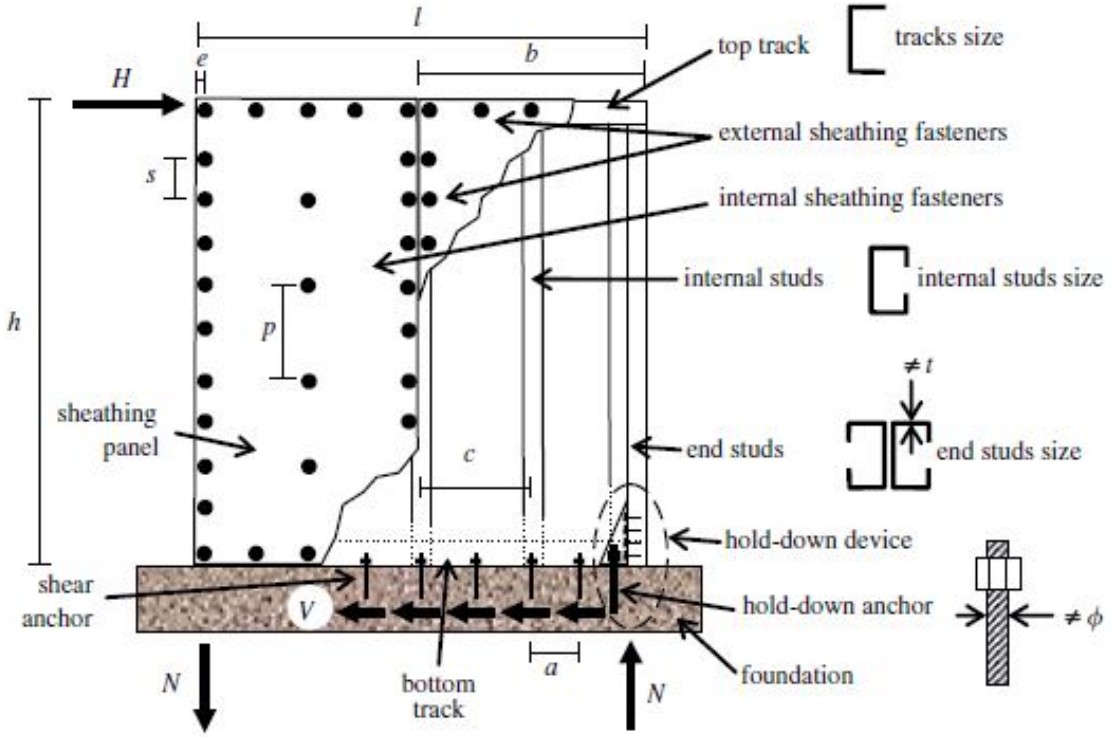

Figure 1.8. Details of a CFS panel (Fiorino *et al.*)

(2009)

stud fastener spacing. Screws, also known as frame to stud fasteners, can be preferred as self-drilling or self-tapping. While tracks are usually selected as U sections, lipped-C or double lipped-C sections can be constructed as stud member. The thickness of the cold-formed steel profiles can be produced from 0.5 mm to 2.5 mm. Since profiles with these thicknesses, in other words, thin-walled steel profiles, plate buckling and cross-section distortion should always be considered in the calculations.

Studs should be anchored with anchor to the foundation with a rod at 120 cm spacing. The foundations are generally constructed as raft foundations, wall-footing type foundation can also be constructed but it is constructed thicker under the outside walls. Anchor device details can be seen below in Figure 1.9.



Figure 1.9. Cold-formed steel with sheathing panel detail [1]

As a result, CFS structures must be resistant to overturning moment and shear forces. As shown in Figure 1.4, the overturning moment is shown as a force couple in the anchors on the bottom track and the axial force strength of the profile should be greater than these. In-plane shear force is countered with both sheathing and sheathing to frame fasteners.

1.3. Literature Review

1.3.1. Existing Codes, Standards and Software

American Iron and Steel Institute (AISI) [4] serves as the voice of the North American steel industry in the public policy arena and advances the case for steel in the marketplace as the preferred material of choice. AISI also plays a lead role in the development and application of new steels and steelmaking technology. AISI S213-07 refers to "North American Standard for Cold-Formed Steel Framing-Lateral Design" and it includes formulation which forms the basis of this thesis.

Turkish Earthquake Code (TEC) 2018 [5] is a specification that includes seismic calculations for buildings in earthquake prone regions. Section 10 and section 15C of

TEC was used in this thesis. Design spectrum and other seismic parameters are also obtained from TEC 2018 [5].

Structural Analysis Program SAP2000 [6] is developed by CSi Computers and Structures company. This analysis program is used during analytical research for this. Both strut model and one-story building model are performed by this program.

ASTM E2126-11 [7] is a specification that requires test methodologies can be called "Standard Test Methods for Cyclic (Reversed) Load Test for Shear Resistance of Vertical Elements of the Lateral Force Resisting Systems for Buildings." Experimental studies were conducted according to these protocols.

1.3.2. Literature Review

Miller and Pekoz (1993) [8] conducted experiments of behavior of cold-formed steel wall stud assemblies under axial loading. Shear wall and vertical studs were examined and the output data were compared to the one given by AISI's [4] "cold-formed 1986" suggestion. It was concluded that some suggestions is given regarding effective length coefficients. The effective length factors Kx and Ky were taken as constant 0.65 for unbraced frame and 0.65 and 0.4 for braced at mid-height of the stud, respectively. Also, the eccentricity was taken attention in this study.

Miller and Pekoz (1994) [9] proposed a research including behavior of gypsum-sheathed cold-formed steel wall studs. A series of axial load tests were performed on GWB panels and these experiments were compared to AISI [4] specification. As a result of these tests, stud spacing was observed to be directly related to the strength. It was clearly seen that as the stud spacing increased strength capacity decreased. Capacity reduction due to stud spacing was also predicted well by specification of AISI [4]. During the tests, failure modes of the frame did not matched with the AISI [4]'s prediction.

Serrette and Ogunfunmi (1996) [10] conducted an experimental study on shear

resistance of gypsum-sheathed light-gauge steel stud walls. This research included three types of shear walls tested according to ASTM E 72-80.

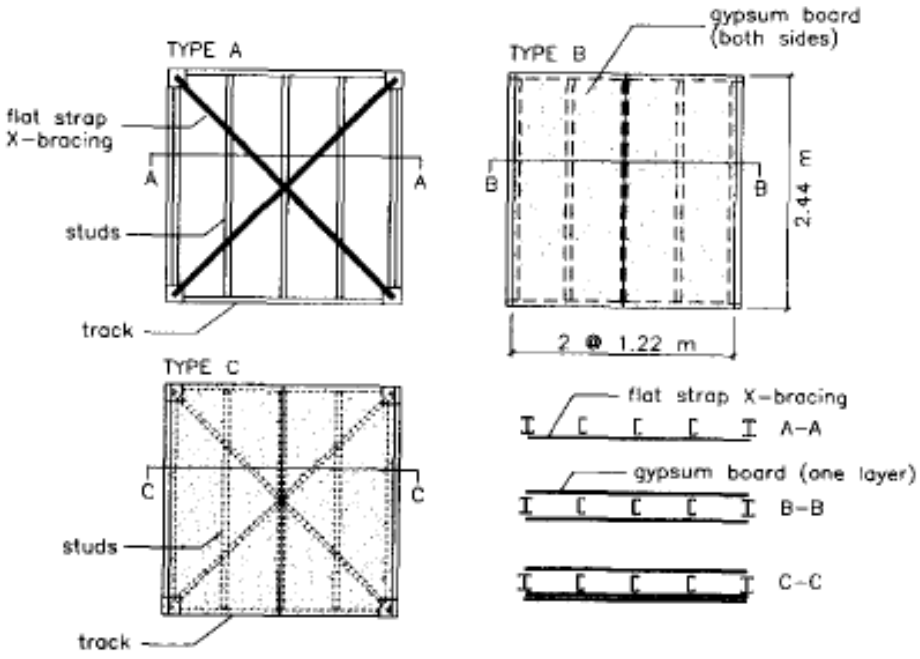

Figure 1.10. Configuration of Type A,B and C Walls

Type A: Stud frame with X-bracing without sheathing, type B: Stud frame with gypsum board without X-bracing and type C: Stud frame with X-bracing and gypsum wall board on the both sides. During the tests, it was concluded that GWB (Gypsum wall board) showed significant lateral capacity. However, some crushing was observed around the screw shank. Using tension bracing, increased the maximum load capacity and increased lateral displacement. Although X- bracing and sheathing showed high shear strength, it was not practical. The author recommended that the portion of shear carried by sheathing need to be limited in order to avoid any fastener to sheathing failure.

Serrette *et al.* (1997) [11] presented a research in order to investigate static racking behavior of plywood, OSB, gypsum and fiber bond wall with metal framing. Three different types of wall: Cold formed steel with sheathed wall, cross-braced wall and truss-braced wall and four different sheathing as plywood, OSB (Oriented Strand Bond), gypsum was used in the experiments. In this study, the effect of screws in

different settlements and different types was examined. It is observed that the fastener type has no effect on maximum strength in plywood system. Also it was concluded that tight spacing with no.8 screws has high strength compared to no.6 screws. Although plywood and OSB were more comparable, gypsum wall board had lower strength. During the full-scale tests, it can be explicitly observed that failure of the walls produced from rotation of the fasteners about the plane of the stud flange followed by either the head of screw pulling though the panel or screw breaking the edge panel. Moreover, in the small scale tests, failure resulted from the fastener breaking the edge of the panel. The comparison full-scale and scale test was performed and it was proposed that small scale test could be used as a simple method.

Rogers *et al.* (2004) [12] conducted an experimental study on a hundred and six cold formed steel framed shear walls which included OSB (Oriented Strand Bond), Douglas Fir Plywood and Canadian Soft Plywood. The main purpose in this research was to develop a guideline for steel frame with shear wood panel walls for use the 2005 National Building Code of Canada (NBCC). Configuration of specimens was as follows: 610x2440 mm, 1220x2440 mm, 2440x2440 mm (length x height). These sheathed walls were tested under cyclic and monotonic lateral loads. As a result, the samples with the configuration of 1220x2440 mm and 2440x2440 mm showed closer lateral deformation whereas the 610x2240 mm sample showed higher lateral deformation while reaching ultimate shear capacities.

Fülöp and Dubina (2004-Part I) and (2004-Part II) [13,14] conducted experimental and numerical study on performance of wall-stud cold-formed shear panels under cyclic and monotonic loading. In the first part of the study, ductility and strengths affecting the behavior of shear walls in different configurations were compared. During the experiments, it was concluded that the panels were important for rigidity and bearing capacity. The hysteretic behavior was characterized by very important pinching and reduced energy dissipation. In addition, failure began through bottom track bolt region. Also, types of failure were discussed at the end of the study.

According to Part-II, a simple finite element model was calibrated to be used

in earthquake simulation modelling. The model was also found to be enough for the purpose of dynamic analyses. Furthermore, there were three levels of performance with corresponding lateral displacement of the walls, while applying the experimentally determined criteria and partial behavior factors were identified for panels based on time-history analysis outputs. The effect of over strength has been observed to be an important source of reduction of the earthquake forces in the post-elastic behavior of the panels. The openings in the walls caused deficiencies in the determination of the elastic boundaries and caused a low shear and deformation capacity. Even if a limited number of seismic forces are used in this study, similar behavioral characteristics can be expected for structures using such elements with lateral strength.

Xu and Martinez *et al.* (2006) [15] conducted an analytical study and compared to an experimental study. Analytical model was presented to state the ultimate lateral strength and lateral displacement of the shear wall panel taking into account geometrical dimension, material properties and construction details such as stud, stud thickness and sheathing to stud fastener size and spacing. According to calculations, one-sided sheathing usually failed from connectors between sheathing to stud and double sided sheathing failed from stud buckling. As a result of the proposed method lateral strength and displacement with different screw spacing, different sheathings or framing materials could be evaluated.

Londolfo *et al.* (2006) [16] conducted tests to investigate seismic behavior of sheathed cold-formed structures. The test specimens were composed of two sheathings. Exterior surface OSB (oriented strand board), interior surface GWB (gypsum wall board) and top surface OSB were formed as a sheathing part of the prototype. One of the prototypes was applied to the monotonic and the other was cyclic load. The conclusions of the experiments revealed that whole components of the construction could be performed according to design criteria, imposing failure or damage in the sheathing to frame connections for vertical wall. In all experiments, the failure of connection screws between the sheathing and stud was observed. In monotonic tests, while increasing in lateral displacement, collapse mechanism was followed by invariant trend after reaching peak values of the lateral load. In cyclic tests, connections at upper

part of the wall were failed earlier than lower part. In addition to this, degradation was seen in peak strength value due to distortional buckling. The lateral load vs. response for displacements was very similar for all tested walls. Before peak value of the strength had been reached, the lateral load vs. displacement responses were nearly the same but essential variations were experienced after the post-peak side.

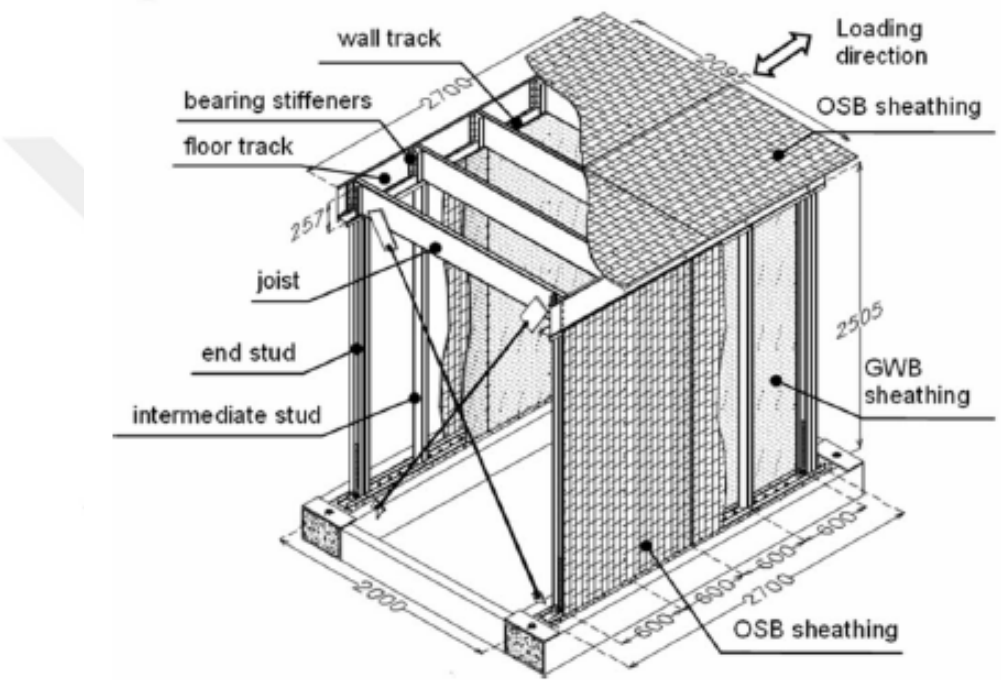

Figure 1.11. 3D view of test prototype

Corte *et al.* (2006) [17] investigated seismic behavior of sheathed cold-formed structures in two parts. The main objective was to investigate whether cold-formed steel structures would be preferred instead of classical reinforcement or masonry structures in this research. To respond this, it was necessary to investigate whether cold-formed steel structures have sufficient strength and ductility. Because of lightness, the low levels of seismic forces could allow the design to be carried out within the elastic field of response according to authors. First of all, mathematical model was developed and hysteresis behavior of CFS wall panels were examined. Then, deformation demand experiments were carried out with 26 ground motion from Italy applied to CFS

wall. As a result, if elastic earthquake design is performed, the inter-story drift would be below the demand damage limit. Also, considering the strength of the walls after the post-break, it can be concluded that the safety of the structure analyzed against collapse is acceptable. These results show that CFS systems can be used instead of masonry or conventional reinforced concrete structures in earthquake-prone countries.

Dubina *et al.* (2008) [18] proposed a research on behavior and performance of CFS framed houses under seismic action. In this study, by examining the past studies, it was combined with its own study. A two story real world structure was constructed to obtain performance and behavior under cyclic and monotonic loading. Furthermore, sheathing to sheathing and frame to sheathing connection tests and in situ ambient vibration tests were conducted to decide how the full-scale structure responded. It was concluded that mounting of OSB did not only increase the rigidity but also changed the weak direction of the construction

Jane and Simsir (2008) [19] conducted a research on nonlinear analysis of wood frame shear walls. In the experiments two walls with two window openings were used. In addition, these wall specimens were coated with gypsum wall board on one side and stucco on the other side. In the experiments, lateral load was applied from the top of the wall to obtain the load vs. displacement graph. The main objective was to create analytical model to represent or simulate the real world structure. Thus, Nonlinear link elements were assigned to model and load vs. deformation property of fastener was represented by SAP2000 [6]. Also, stucco and drywall was represented as a shell element in this program. It has been concluded that load vs. displacement values obtained from test samples and structural model were found to be very convergent.

Fiorino *et al.*(2009) [20], Landolfo et al. (2010) [21] have proposed a study about a seismic design procedure for sheathed cold-formed steel housing. According to authors, a huge number of experimental and theoretical studies are presented, these studies still need some improvement in the domain of seismic design. As an attempt to develop some calculations and some nomographs, this stud aims to present a structural design procedure. Thus, three different phases have been adopted for this design procedure:

- Definition the sheathed wall parameters (spacing of the studs c, height of wall h) and some other parameters of the wall components: Sheathing (type, thickness, orientation), frame (stud size, steel grade, track size), sheathing to frame connections (interior spacing p, fastener type, edge distance e), type of hold-down anchors and shear anchors
- Evaluation of the sheathing-to-frame fastener exterior spacing (s)
- Evaluation of other parameters (stud thickness t, hold-down anchor diameter Φ, shear anchor spacing)

The first phase does not depend on the seismic design; they can be determined from architectural or technological choices and design for vertical loads. Furthermore, exterior spacing s (phase 2) and phase 3 can be derived from seismic analysis. This seismic analysis includes linear dynamic (LD) seismic procedure and nonlinear static (NS) seismic procedure that can be seen in Figure 1.12 and Figure 1.13.

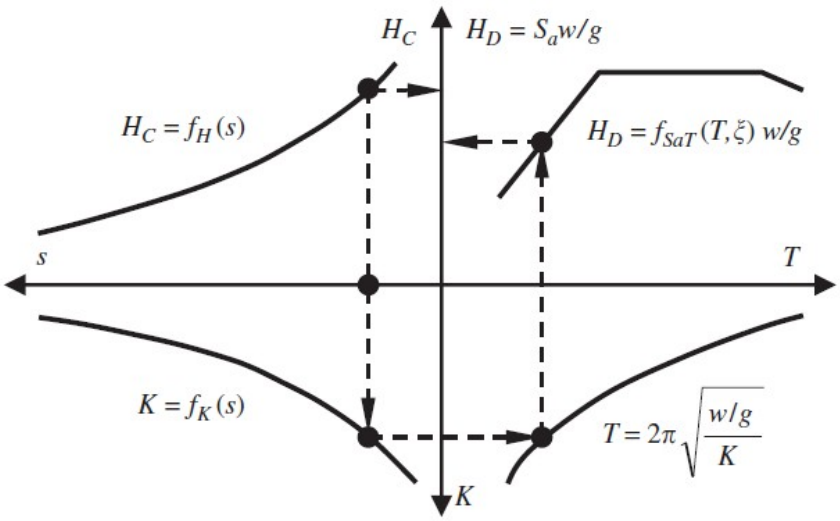

Figure 1.12. LD Nomographs

In LD seismic procedure, a force-based design approach is used. Besides, inelastic behavior and the structural over-strength are considered by seismic force modification factors. LD seismic procedure can simply be summarized utilizing the nomograph demonstrated above. Depending on s, stiffness (k) and Resistance (Rr) can be obtained. According to the stiffness computed, period (T) is found out knowing the

seismic action demand from Equation 1.1

$$H_D = S_a \frac{w}{g} \tag{1.1}$$

Spectral acceleration (S_a) can be acquired as a function of T and viscous damping ratio (ξ). That means seismic strength capacity can be compared to seismic action demand and this procedure is followed till performance and monetary considerations are satisfied Equation 1.2

$$H_C \geq H_D \tag{1.2}$$

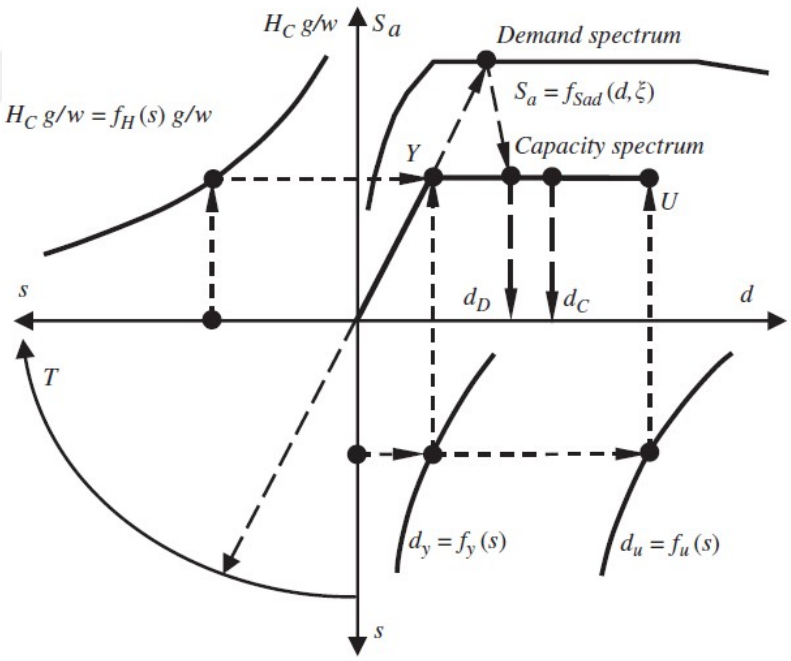

Figure 1.13. NS Nomographs

In NS seismic procedure, a displacement-based approach is used. The inelastic behavior and the structural over-strength are directly considered in this procedure. NS seismic procedure can simply be summarized utilizing the nomograph demonstrated above. Comparison of seismic displacement capacity to that of demand can readily

be performed taking advantage of this nomograph (acceleration-displacement spectrum) which involves both demand and capacity spectra. Spectral acceleration can be obtained as a function of spectral acceleration (f_{Sad}) with respect to the generic displacement (d) and viscous damping ratio (ξ).

$$S_a = f_{Sad}(d, \xi) \tag{1.3}$$

Capacity spectrum is sketched as an elastic-plastic curve which is determined by the yield (Y) and ultimate (U) limit points:

$$Y(d_y, \frac{H_c}{w}g), \qquad U(d_u, \frac{H_c}{w}g) \tag{1.4}$$

where the yield displacement (d_y) and ultimate displacement (d_u) can be obtained as a function of the exterior spacing (s) can be seen in the Equation 1.5.

$$d_y = f_y(s), \qquad d_u = f_u(s) \tag{1.5}$$

Utilizing the LD Nomograph, for certain values of exterior spacing (s), involvement of the computable functions f_{Sad}, f_H, f_y and f_u as well as fixed quantities of seismic weight (W) and viscous damping ratio (ξ) will provide the design procedure with calculating both seismic demand (d_D) and capacity (d_C). That means seismic displacement capacity can be compared to seismic displacement demand and this procedure is followed till performance and monetary considerations are satisfied.

$$d_C \geq d_D \tag{1.6}$$

After determining sheathing-to-frame fastener exterior spacing (s), the evaluation of stud thickness (t), hold-down anchor diameter (φ) and shear anchor spacing (a)

should be determined to complete the design.

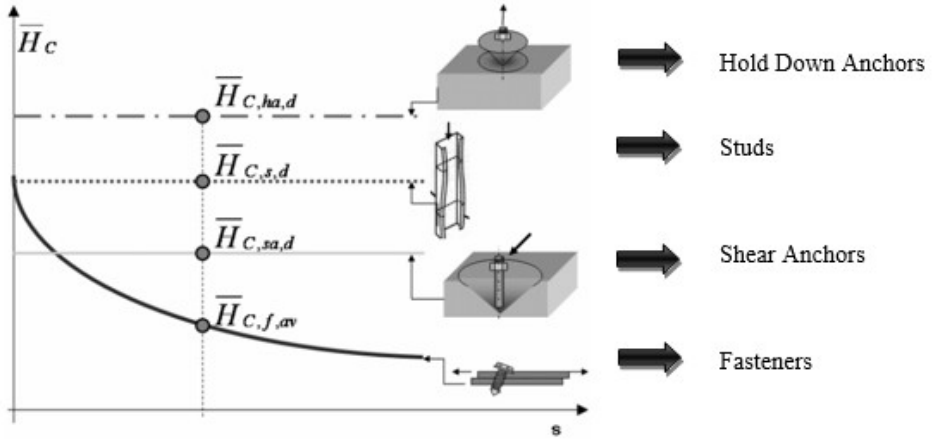

Figure 1.14. OC Nomographs

The nomograph presented in Figure 1.14 represents the wall shear strength per wall unit length (H_C) corresponding to the resistance of sheathing fasteners ($H_{C,f}$), studs ($H_{C,s}$), hold-down anchors ($H_{C,ha}$) and shear anchors ($H_{C,sa}$). They are represented together as function of the exterior spacing (s).

$$\bar{H} = f_H(s),\ \ \bar{H}_{C,S} = \frac{H_{C,S}}{l} = \frac{N_s}{h},\ \ \bar{H}_{C,ha} = \frac{H_{C,ha}}{l} = \frac{N_{ha}}{h},\ \ \bar{H}_{C,sa} = V_{sa}(\frac{1}{a} + \frac{1}{l}) \quad (1.7)$$

where N_s is the stud compression axial strength, N_{ha} is tension axial strength of hold-down anchor and V_{sa} is shear strength of the shear anchor.

$$\frac{\bar{H}_{C,s,k}}{\gamma_{ov,s}} \geq \bar{H}_{C,f,d},\quad \frac{\bar{H}_{C,ha,k}}{\gamma_{ov,ha}} \geq \bar{H}_{C,f,d},\quad \bar{H}_{C,f,d},\quad \frac{\bar{H}_{C,sa,k}}{\gamma_{ov,sa}} \geq \bar{H}_{C,f,d} \qquad (1.8)$$

where $\bar{H}_{C,s,k}$ is shear characteristic strength of stud per wall unit length, $\bar{H}_{C,ha,k}$ is shear characteristic strength of hold-down anchors per wall unit length, $\bar{H}_{C,sa,k}$ is shear characteristic strength of shear anchors per wall unit length $\bar{H}_{C,f,d}$ is shear design strength of sheathing fasteners per wall unit length, $\gamma_{ov,s}$ is overstrenght factor of studs, $\gamma_{ov,ha}$ is overstrenght factor of hold-down anchors and $\gamma_{ov,sa}$ is overstrenght factor of shear anchors.

Making use of the OC Nomograph presented in Figure 1.14, for certain values of

exterior spacing (s), the design parameters of interest (t, a and ϕ) can be obtained till the "Capacity Design" criteria are satisfied.

The applications done so far in this article demonstrated the design of CFS housing requires definition of the wall shear response (f_k , f_H , f_y and f_u) as a function of exterior spacing (s). In LD seismic analysis, only wall stiffness f_k and strength f_H must be defined, whereas in application of NS procedure, the definition of the elastic-plastic curve through the functions f_H , f_y and f_u needs the acquisition of whole force (H) - displacement (d) response curve of the wall. For this purpose, a specific analytical-numerical method has been developed by the authors allowing the prediction of the whole curve in terms of f_k , f_H , f_y and f_u. According to this methodology, the lateral displacement of a sheathed CFS shear wall can be obtained by adding four different deformation contributions as shown in Equation 1.9.

$$d = d_f + d_s + d_b + d_a \tag{1.9}$$

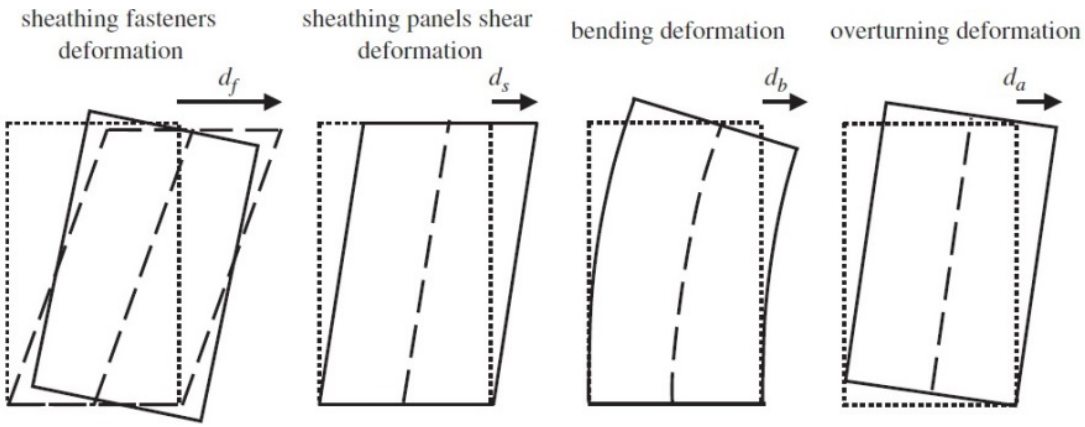

Figure 1.15. Deformation Component of a Sheathed CFS Shear Wall

The conclusions show that the best performance of CFS housing systems is obtained when sheathing-to-stud screw failure is generated. To assure this, a design procedure has been proposed in this article. After determining the shear wall geometry

and technological components, the exterior spacing of the fasteners (s) is determined utilizing LD seismic analysis or NS seismic analysis. Finally all other parameters such as studs, shear and hold-down anchors are obtained. As a final step, analytical model used to define the wall strength curves is presented.

Schafer *et al.* (2010) [22] presented an article about computational modeling of cold-formed steel. Elastic buckling and nonlinear collapse analysis has performed and mesh type effect also investigated with various FEM programs. Factors that determine the solution's accuracy was specified. It was also stated that solver intensity, element choice, discretization, boundary conditions, initial residual stress, initial imperfections should be considered in the collapse mechanism. Fine mesh and medium mesh was enough for local, distortional and global buckling modes.

Landolfo *et al.* (2012) [23] proposed a study about seismic analysis of sheathing-braced cold-formed steel structures. It was stated in the research that shear wall determines the lateral response and behavior of CFS structures. According to authors, if a CFS structure with sheathed wall was designed according to "sheathing-design" method, the structure would be characterized with nonlinear response of the sheathing to frame connectors and a strong pinching of hysteric loops. In this study, the authors examined a single-story building and which behavior factor should be used in structural performance. Finally, a seismic design procedure that allows the evaluation of the external screw spacing with non-linear dynamic analysis results was presented. The feasibility of the procedure is shown by the design of a typical single-story house in the area of medium seismicity. Case study results confirm that an "enhanced objective" design approach is only possible with a small reduction of screw spacing.

Peterman *et al.*(2014) [24] presented an article about hysteretic behavior of the correction between cold formed steel (CFS) studs and sheathing when subjected to in-plane lateral demands. The experiment was performed according to both monotonic and cyclic (CUREE) protocols. Fastener spacing, sheathing types such as GWB (gypsum wall board) and OSB (oriented strand board) and stud thickness were stated variable. As a result of monotonic tests, lateral strength and stiffness for a fastener

in OSB were far greater than GWB. Eventually, not only the shear strength but also stiffness and failure mode were affected by sheathing type. Moreover, as a behavior of connection of stud to sheathing, pull through was dominant for OSB and bearing is dominant for gypsum.

Peterman and Schafer (2014) [25] conducted a research to investigate sheathed CFS (cold formed steel) studs under axial and lateral load applications. Bare frame (unsheathed frame), only one-sided OSB or GWB sheathed frame and both-sided OSB or GWB sheathed frame were tested in this experiments. It is concluded that, sheathings were very vital to stabilize and make strong for studs. The unsheathed studs failed in a torsion limit state. The One-sided sheathing had a greater capacity but was still unsatisfactory from twist and pull-through of the fasteners through the sheathings. GWB sheathed specimens exhibited more damages around the fastener and were not able to reach full member capacity. In addition, the strength in fastener limit states was estimated by a new computational model. Finally, torsion, bearing and pull-through limit states were converged with the obtained test results.

Asteris *et al.* (2015) [26] presented an article about a macro-modelling approach for the analysis of infilled frame structures considering the effects of openings and vertical loads. In this study, equivalent strut is used instead of infilled frame with different size of openings.

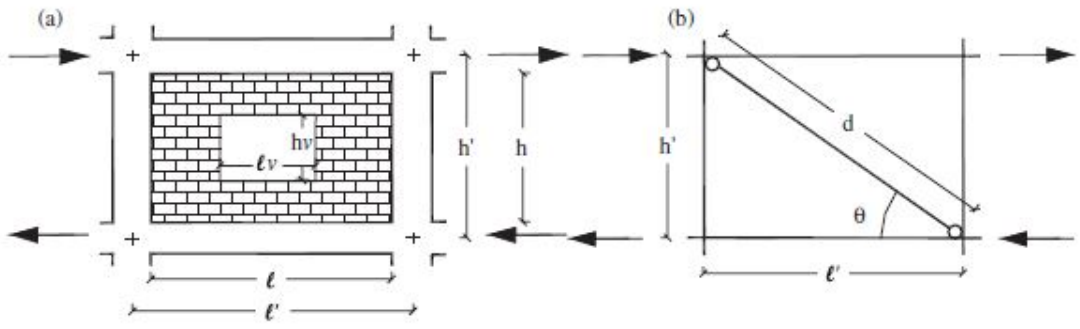

Figure 1.16. An infilled frame under lateral load: (a) actual system, (b) macro-model

The lateral stiffness D_i of the simplified model and can be obtained as the sum of the lateral stiffness of bare frame D_f and lateral stiffness of the pin jointed braced frame D_d can be calculated with Equation 1.10.

$$D_d = \frac{1}{\delta_{p1p2}} = \frac{k_d(\cos\theta)^2}{1 + \frac{k_d}{k_c}(\sin\theta)^2 + \frac{k_d}{k_b}(\cos\theta)^2} \tag{1.10}$$

where k_c, k_b and k_d are the axial stiffness of the column, beam and diagonal strut, respectively.

$$k_d = \frac{E_d t_w}{d} \tag{1.11}$$

$$k_c = \frac{E_f A_c}{h'} \tag{1.12}$$

$$k_d = \frac{E_f A_b}{l'} \tag{1.13}$$

where E_d and E_f are the Young's modulus of the strut and frame,respectively; t, w and d are thickness, width and diagonal length of the infill wall, respectively; A_c and A_b are the cross section are of the column and beam; θ is the angle between strut and horizontal; and h' and l' are the height and length of the infilled frame.

The other parameters D_f and D_i are explained by Equation 1.14 and Equation 1.15, respectively.

$$D_f = \frac{24E_f I_c}{h'}(1 + \frac{l' I_c}{h' I_b}) \tag{1.14}$$

$$D_i = D_d + D_f \tag{1.15}$$

where I_b and I_c are the moments of inertia of beam and column sections, respectively.

In case of different cross sections of the column, mean value of their axial stiffness can be used.

A number of numerical investigations were performed by changing the l / h ratio and changing the opening ratio of the infilled frame. As a result of the investigations, area of the opening changes the deformed shape of the infilled frame. The infilled frame with no opening gives a contribution to lateral stiffness; on the contrary, huge opening gives a negligible stiffness. The variables in the formulas given to determine the equivalent strut width are interdependent and there is no linear relationship between them and this is the result of the interaction between infilled wall-column and infilled wall-beam.

Karabulut and Soyoz (2017) [27] have conducted experimental and analytical studies on different configurations of cold-formed steel structures.

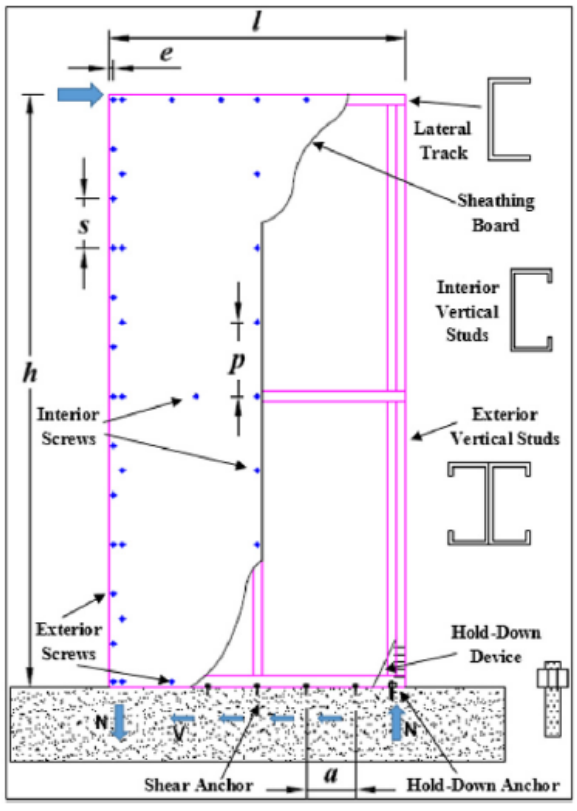

Figure 1.17. Components of a typical CFS shear panel

A bunch of experiments have conducted at Structure Laboratory of Boğaziçi University. Experiments were conducted to obtain the damage formation, and to compute lateral load resisting capacity as well as strength reduction factor(R) which can all provide significant information for the seismic performance of these shear panels. A few kinds of test specimens were tested as shown in the Table 1.1.

Table 1.1. List of CFS shear panels

Types of specimens	**Steel thickness (mm)**	**Sheathing type**	**Screw spacing external/ internal(mm)**	**Axial Load (ton)**	**No of Tests**
Type 1	0.9	Board Type 1	200/300	-	3
Type 2	0.9	Board Type 2	200/300	-	3
Type 3	1.5	Board Type 2	200/300	-	3
Type 4	0.9	Board Type 1	150/300	-	1
Type 5	0.9	Board Type 1	100/300	-	1
Type 6	0.9	Board Type 1	200/300	1.2	2
Type 7	0.9	Board Type 1	200/300	2.4	2
Type 8	0.9	Board Type 1	200/300	4.9	1

Two types of steel thicknesses, two types of gypsum wall board and three different screw spacing configurations were used in those experiments. Board type 1 is made from specially calcined high purity natural gypsum that provides lightness, hardness, resistance and workability to plasterboard and board type 2 is made same material with board type 1; in addition, the board type 2 is reinforced with fiberglass because it is considered an external wall.

After experiments, the most convergent mathematical model was found to create one-story building. This one-story building was investigated in terms of seismic performance assessment.

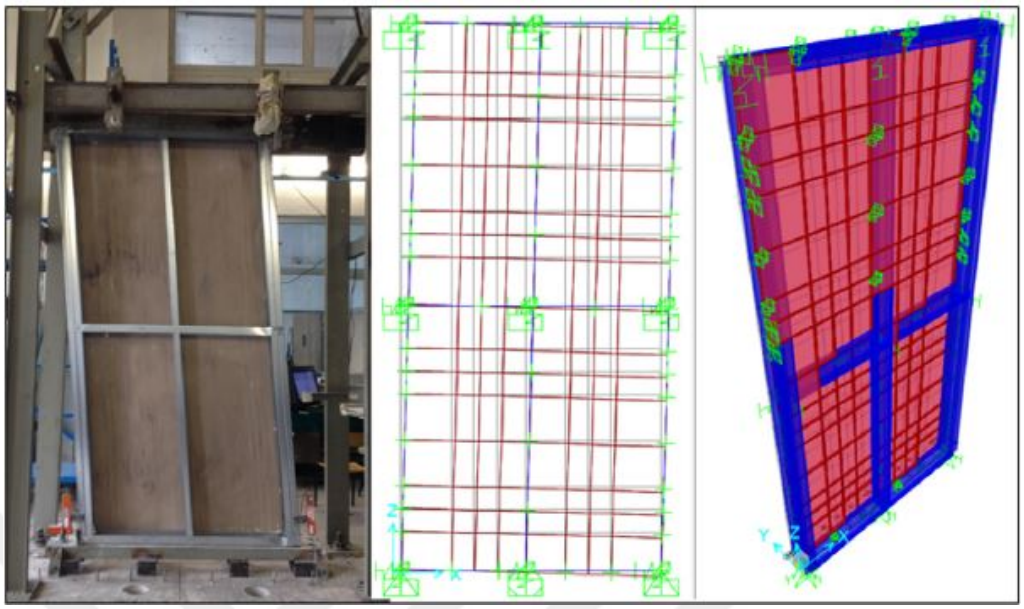

Figure 1.18. CFS panel and its analytical model of a CFS panel

As a result of these studies, screws have a great role on the energy absorption capacity. Increasing or decreasing spacing of the screws directly affects the lateral load capacity of the panel. Reinforcing the board like board type 2 with a fiberglass has a positive impact on the panel as increasing the shear capacity and stiffness. It can be noted that CFS structures in earthquake-prone regions such as Turkey have satisfactory performance.

1.4. Scope and Motivation of the Thesis

CFS structures are used in countries such as USA, Japan, Germany, Great Britain and Australia, however, its construction become widespread all over the world after publication of the AISI [4] specification. Today, many countries are using light steel construction systems and improving their specifications.

The load-bearing system of the cold-formed steel structures is generally formed by cold-formed steel studs, tracks and various sheathings such as gypsum, OSB, metal sheet and plywood. Cold-formed steel construction systems have been an alternative in the construction marketing in terms of cost and time. Unlike conventional construc-

tions, cold-formed steel structures are much more environmentally friendly, especially for the cold-formed steel profiles being a hundred percent recyclable, which is a good advantage for consumers. Other upsides of the cold-formed steel structures are low weight, easy applicability, low cost and less construction time. Due to these features, cold-formed steel structures have become more popular day by day.

On the other hand, some disadvantages of cold-formed steel construction systems can be stated. Cold-formed steel members have particularly very low thicknesses and this may cause some structural instability. Cold-formed steel members can be easily faced to local buckling, global and distortional buckling need to be taken precautions. Cold- formed steel construction systems also require detailed sheathing systems in order to protect against temperature changes. Sheathing types are very vital in terms of shear resistance in these structures. Shear capacity and reaction of the structures can directly change according to each type of sheathing. Therefore, many researchers work in this field to improve the calculation methods. Due to the increasing popularity of the cold-formed steel structures, countries are developing their own specifications.

Turkey is one of the countries where the popularity of cold-formed steel building systems has increased in recent years. Turkey is in an earthquake-prone region and should have stocks of cold-formed steel structures. Light-gauge steel elements previously used in the industrial area became widespread in the housing after the earthquake.

The experiments carried out at Boğaziçi University Structural Laboratory in 2015, it has been featured in the 10th section of the Turkish Earthquake Code 2018 [5]. The results of some of these experiments were used in this thesis and are included in Chapter 2. In these experiments, lateral load displacement values were obtained by using various screw spacing and different steel thicknesses.

Cold formed shear panel basically consists of sheathing, cold-formed steel profiles and screws. Sheathing is fastened the cold-formed profiles by the screws. Screw spacing directly affect shear strength of the structure. In order to estimate the behavior of these

panels under earthquake loads, live loads and dead loads, engineers should define the every screw as link element in each spacing. However, this takes a lot of time from users.

Main objective of the thesis is to replace gypsum sheathing with a diagonal strut in order to save the time and analytical model complexity. Considering the lateral force and lateral displacement values in the test results, the equivalent diagonal strut model is represented instead of the shear panel. The diagonal strut width is determined and assigned to analytical model in the computational program SAP2000 [6]. The equation for strut width is given in Section 3.8.

In this thesis, diagonal strut is used instead of GWB (gypsum wallboard) and the width of this diagonal strut is expressed by a suggested equation for convenience. This suggestion is exemplified with a one-story structure and results are listed in the conclusion part.

1.5. Thesis Overview

This thesis consists of five chapters and the contents of these chapters are as follows. Chapter 1 is the introduction part of the thesis. This section provides a general framework for cold-formed steel structures. It also includes content of the thesis, thesis objective and literature survey. Chapter 2 is about the experimental study which is completed in the Structural Laboratory of Boğaziçi University. It also includes test results. Chapter 3 is presents the diagonal strut width calculations. Formulas are proposed by comparing the experimental results and the analytical model. In Chapter 4, one-story structure is modeled incorparating struts instead of the gypsum board. Sheathing and stud performances under loads affecting this structure are examined. Chapter 5 present the conclusion of the thesis and proposal future works.

2. EXPERIMENTAL STUDY ON VARIOUS CFS SHEAR PANELS

2.1. Introduction

A dozen tests were carried out at the Boğaziçi University in Structure Laboratory to determine the behavior of the panel, which consists of a cold-formed steel frame and sheathing under horizontal load. The behavior of light steel buildings under earthquake loads was tried to be determined with these tests. As a result of these experiments, TEC 2018 [5] Chapter 10 was presented. The results of some of these experiments were also used in this thesis.

2.2. Configuration of Shear Panel

Shear panel consists of screws, studs and tracks as seen in figure 2. Lipped double C section is located on the both edge of the panel and single lipped C section is positioned in the center of the panel. The tracks consist of unlipped C profiles and 12.5 mm thick gypsum board was used as sheathing. This gypsum board is connected to the steel profiles at 100,150 and 200 mm spacing at the edge. However, it is always fixed to steel profiles at 300 mm intervals in the middle of the panel. Cold-formed steel cross sections used in these experiments can be seen in Figure 2.1 and panel details can be seen in Figure 2.2.

2.3. List of Shear Panels

Each set of shear panels consists of three experiments and the number of samples and samples used in this thesis are given in Table 2.1. Two different steel specimens of 0.9 and 1.5 mm thickness were used. There are 3 different test sets of 0.9 mm thick steel with 100, 150 and 200 mm screw spacing. The panel, which is formed of 1.5 mm thick steel, has a 3-set test set with 200mm screw spacing.

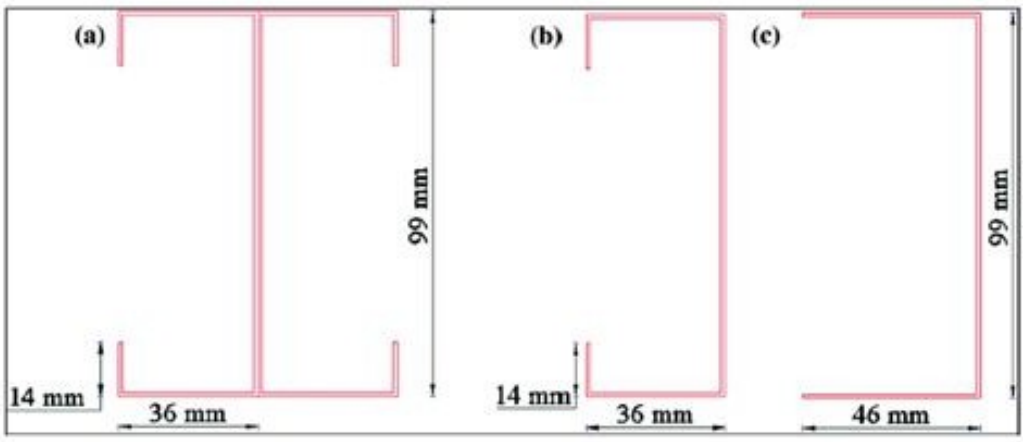

Figure 2.1. Cross sections of cold formed steel members

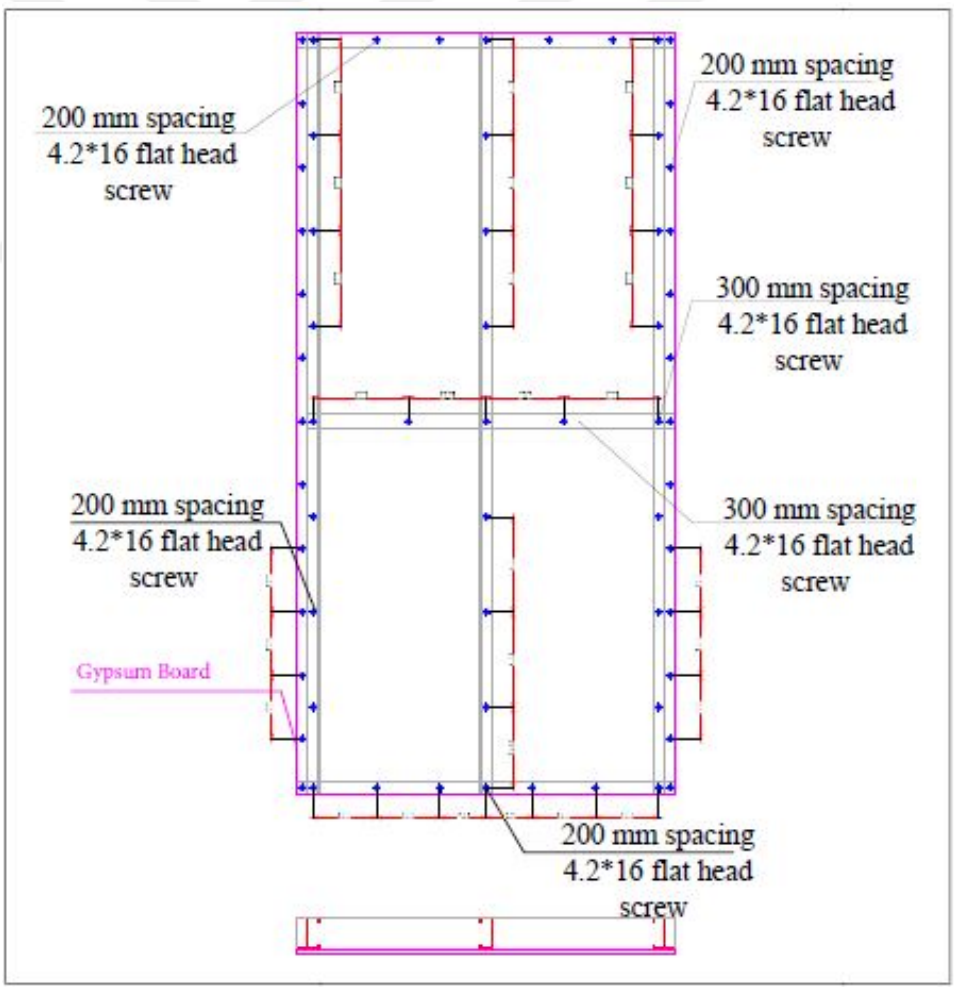

Figure 2.2. Configuration of shear panel

Table 2.1. Shear Panel Specimens

Wallboard Type	**Steel thickness (mm)**	**Screw spacing (mm)**	**Number of experiments**
GWB	0.9	100	3
GWB	0.9	150	3
GWB	0.9	200	3
GWB	1.5	200	3

2.4. Loading Protocol and Loading Frame

The experiments were conducted at Boğaziçi University in Structure Laboratory. While testing all panels, Dartec brand hydraulic actuator which has 25 tons of capacity was used. This mechanism has been very useful in measuring horizontal load and displacement. The Hydraulic actuator and test assembly are also shown in Figure 2.3.



Figure 2.3. Hyraulic Actuator and Reaction Frame

In ASTM E2126-11 [7] , also used by AISI [4] as the loading protocol, "Standard Test Methods for Cyclic (Reversed) Load Test for Shear Resistance of Vertical Elements of the Lateral Force Resisting Systems for Buildings protocol. Experimental steps and cycle numbers according to this protocol are given in Table 2.2 and Figure 2.4.

Table 2.2. Test Steps and Number of Cycles

Step	**Number of Cycles**	**Amplitude of Primary Cycle,(% Dmax)**
1	6	5
2	7	7.5
3	7	10
4	4	20
5	4	30
6	3	40
7	3	70
8	3	100
9	3	100+5
10	3	Additional increments of 50 (until specimen failure)

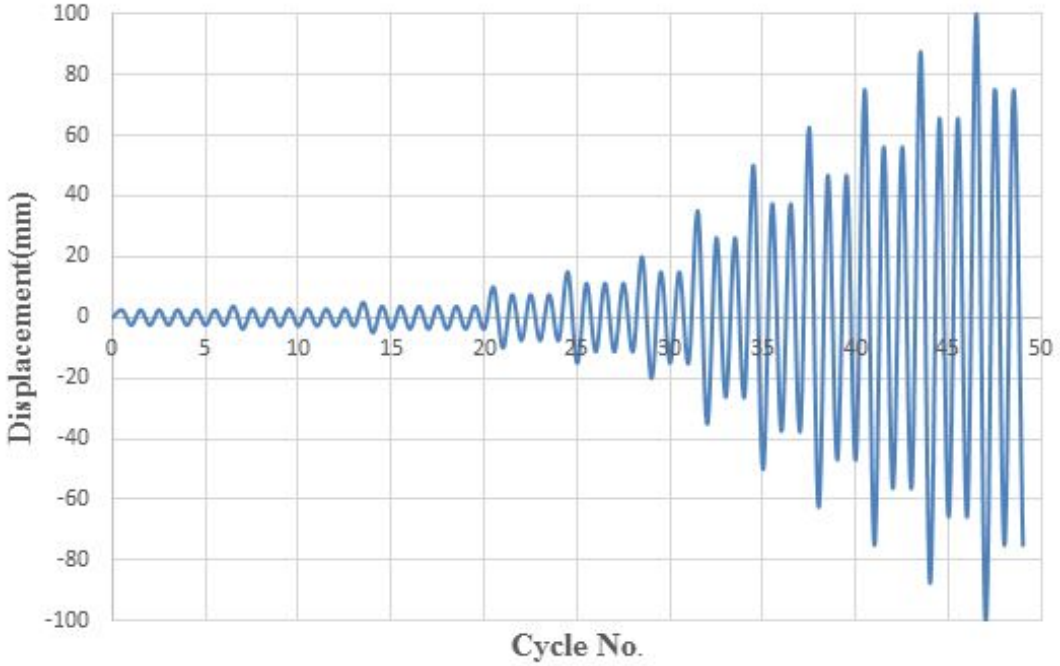

Figure 2.4. Test Steps and Number of Cycle

Based on the same references, the following rules regarding the loading protocol have also been applied.

- The size of the cycles after the first cycle in each step was taken as 75% of the size of the first cycle. Dmax is the largest predicted displacement and is obtained at the point where the force applied in the first cycle does not drop below 80% of the maximum force obtained during the test.
- The Dmax value can also not be greater than 2.5% of the panel height.
- Loading can be in the speed range of 1.0-63.5 mm / sec.
- The collapse of the panel is considered to be 0.8 of the ratio of the applied force to the largest force.

2.5. Test Results

2.5.1. Test result of the Panel with 0.9 mm steel thickness and 100-150 mm screw spacing

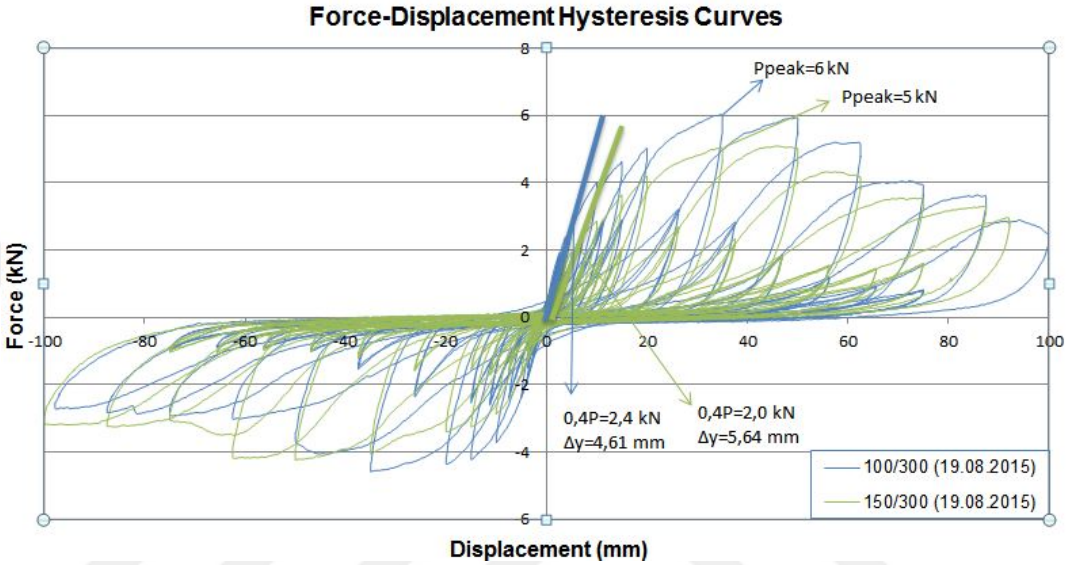

Figure 2.5. Experimental results of the Panel with 100 and 150 mm screw spacing

2.5.2. Test result of the Panel with 0.9 mm steel thickness and 200 mm screw spacing

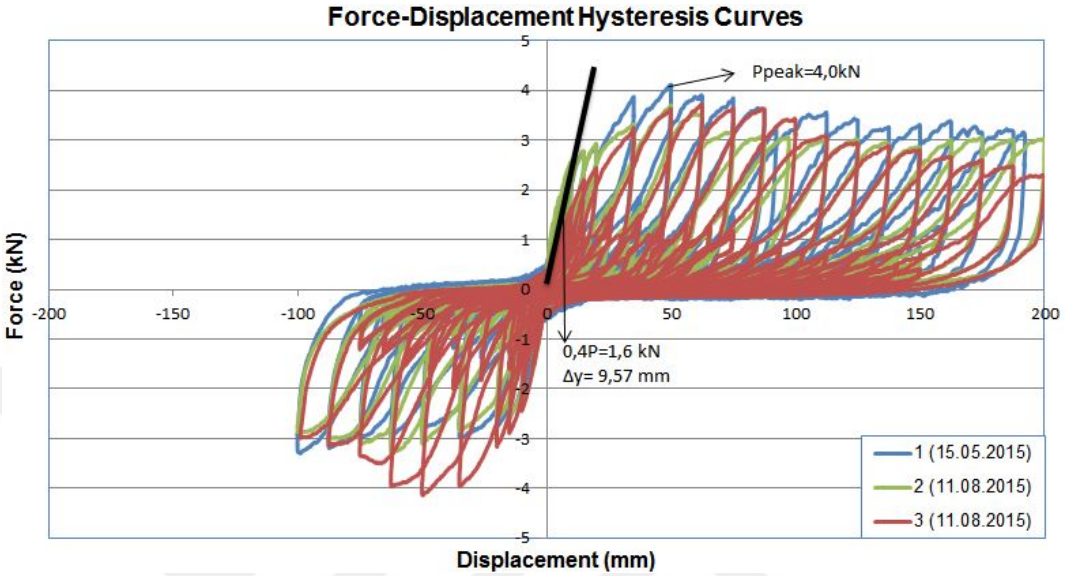

Figure 2.6. Experimental results of the Panel with 200 mm screw spacing

2.5.3. Test Result of the Panel with 1.5 mm steel thickness and 200 mm spacing

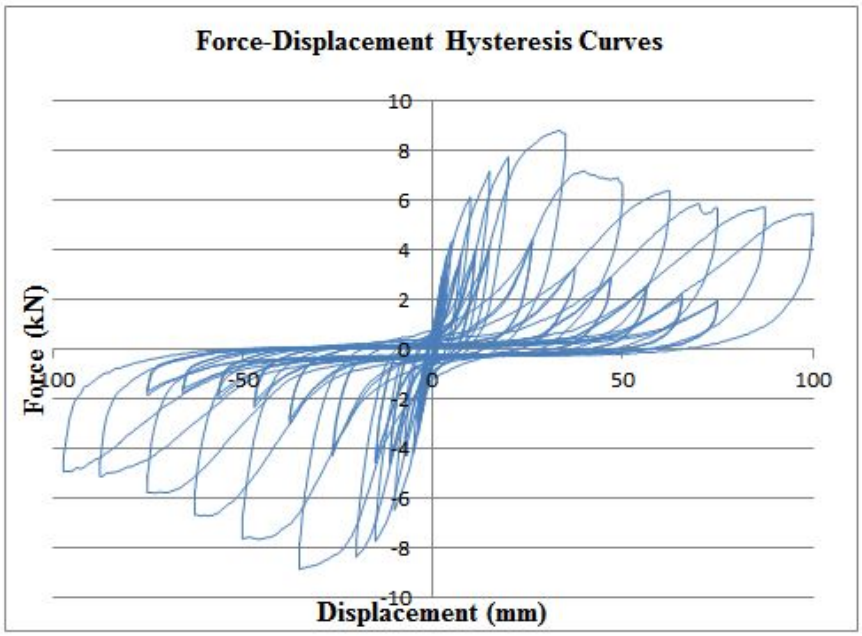

Figure 2.7. Experimental Results of the Panel with 200 mm and 1.5 mm steel thickness

2.6. Photos of the Experiment

Experimental photographs are included in this subject in terms of visualization of failure types. Details can be found in Soyoz *et al.* [27].



Figure 2.8. Deformed CFS panel after loading



Figure 2.9. Damage observed at peak displacement of 50 mm



Figure 2.10. Damage observed at peak displacement of 100 mm

3. ANALYTICAL STUDY ON EXPERIMENTAL VALUES

3.1. Introduction

The analytical model of test specimens is a very complex task. As shown in Figure 3.1, each element must be modeled to obtain close value compared to experimental studies. The link elements assigned instead of the screw elements have a vital effect on the panel behavior. Estimating, optimizing and assigning the parameters of the link elements to the model require detailed calculations. Therefore,a method which is suggested to engineers as an ease of calculation, is explained in the following sections.

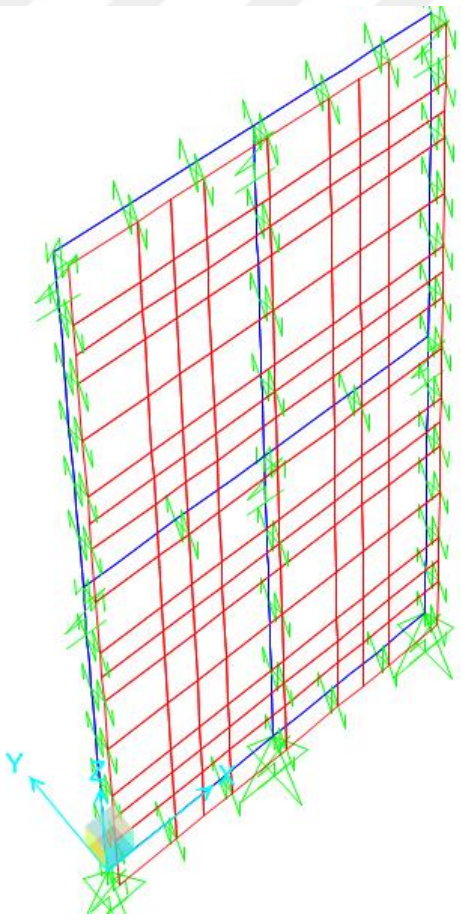

Figure 3.1. A completed analytical model of the CFS panel

As can be seen in Figure 3.1, a meshed gypsum wall board is represented by red

lines, green parts on the frame are link elements which represent screw and blue parts are the cold-formed steel sections. Also shown that the CFS panel is simply supported at three points.

All of this difficulty and complexity can be solved by using the model seen in Figure 3.2 instead of Figure 3.1. Track and stud which are located in the middle of the panel are demolished. Furthermore, a diagonal strut is placed as seen in Figure 3.2.

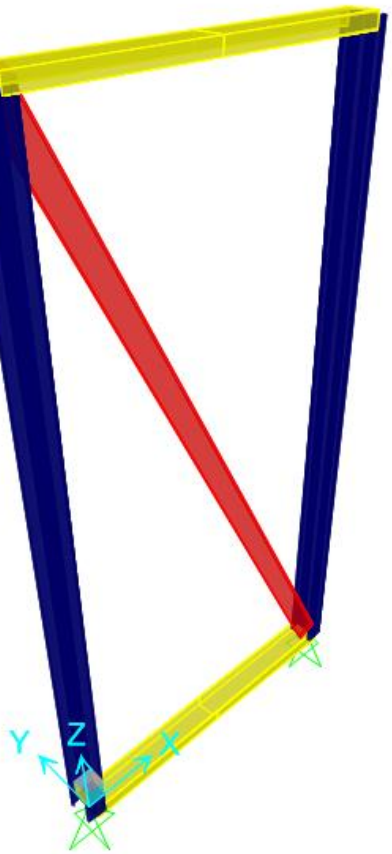

Figure 3.2. An extruded view of the analytical diagonal strut model

where blue parts are studs, yellow parts are top and bottom tracks and gypsum wallboard is represented by the red part called an equivalent diagonal strut.

3.2. The Basis of the Analytical Approach

At first, it is necessary to capture the applied force and resultant displacement values to see whether the results of the experiments match the newly created equivalent strut model or not. In this context, it is necessary to examine the basis of the system first to understand how the frame reacts to lateral force. The force vs. displacement values obtained from the experiments and obtained analytical model should be very close in order to find the strut width to represent the whole wallboard. A typical sketch of the analytical model can be seen in Figure 3.3.

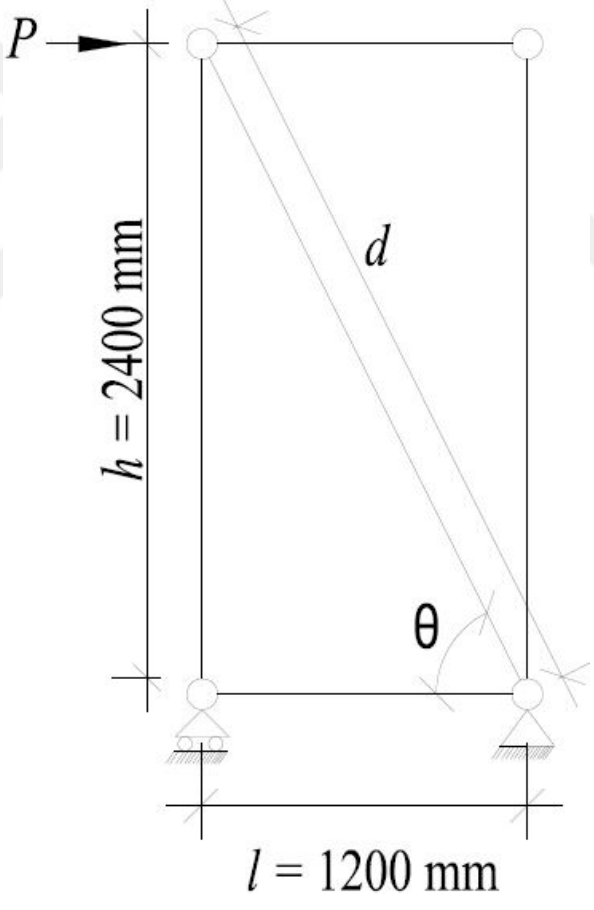

Figure 3.3. A typical sketch of the analytical strut model

where P is the applied load, d is the diagonal strut length, θ is the angle between track and strut, h is the height of the frame and l is the length of the frame.

In order to calculate the stiffness D_d, interstory drift referred to the middle span

of the tracks is first calculated under a unitary lateral load in agreement to the Figure 3.4.

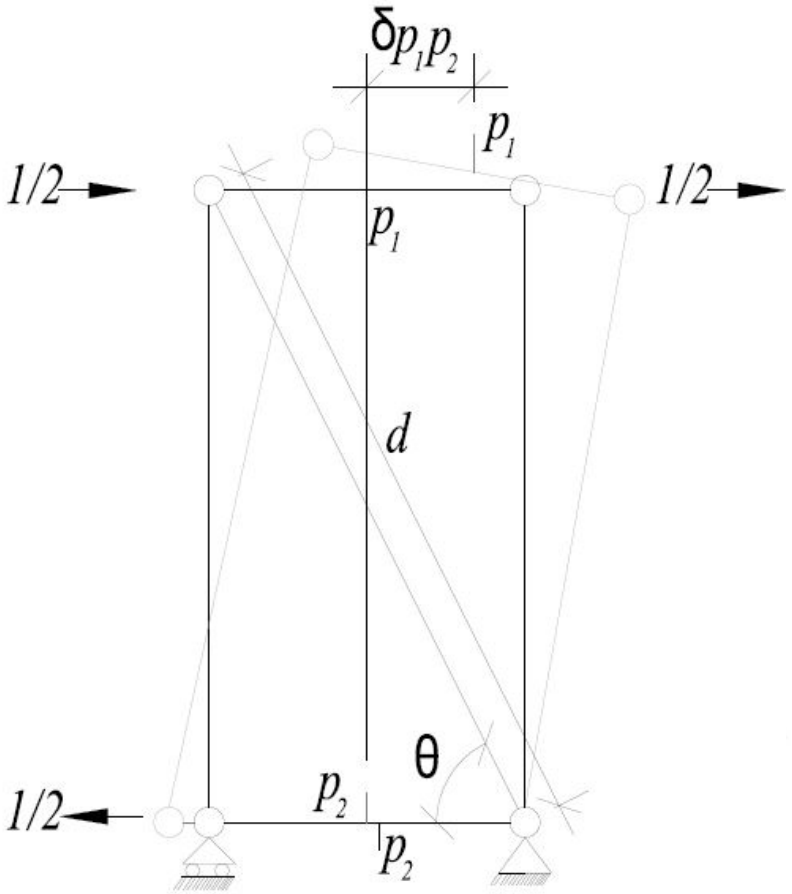

Figure 3.4. Deformed shape of the unit

The inverse of this displacement is the investigated stiffness. Thus, interstory displacement δ_{p1p2} can be stated by Equation 3.1.

$$\delta_{p1p2} = \delta'_{p1p2} + \delta''_{p1p2} \tag{3.1}$$

where δ'_{p1p2} and δ''_{p1p2} are the mean interstory displacements calculated in the middle span of the tracks can be seen in Figure 3.5 and 3.6, respectively.

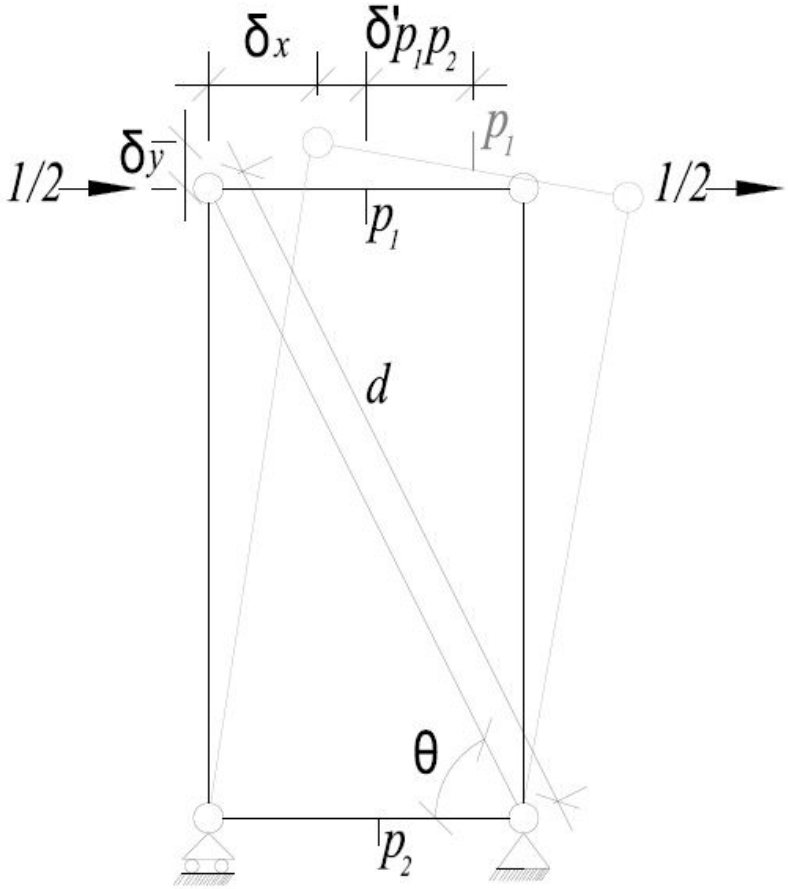

Figure 3.5. Deformation under top load

As can be seen in the Figure 3.5, displacement at mid-span can be expressed as follows:

$$\delta'_{p1p2} = \delta_x + \delta_{p1} \tag{3.2}$$

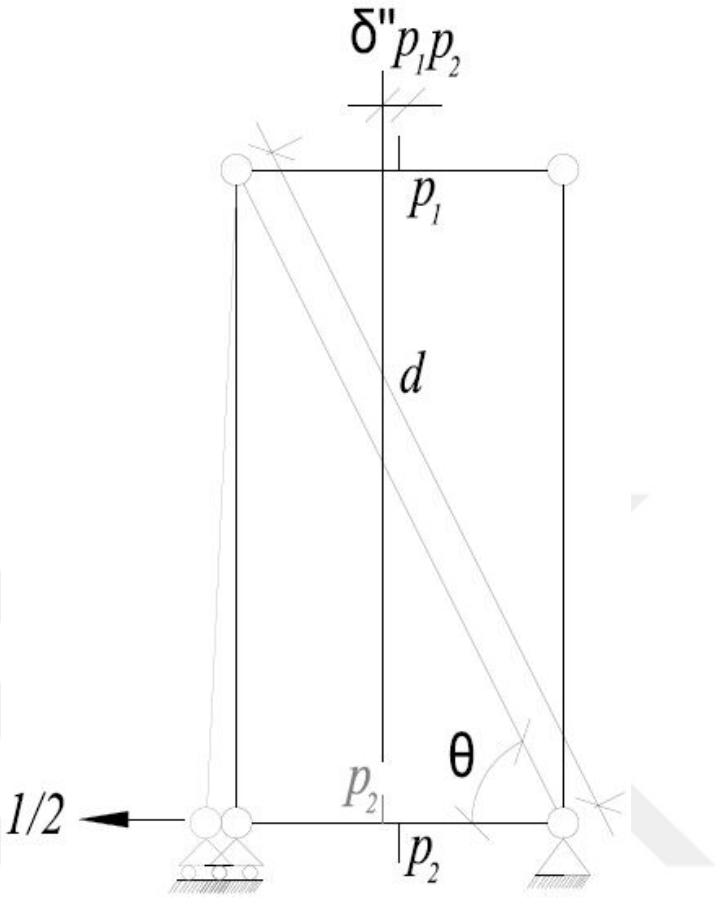

Figure 3.6. Deformation under bottom load

where δ_{p1} is the elongation of the of the upper track calculated at the mid-span. The axial forces in the members given in Figure 3.6 can be stated by Equation 3.3, 3.4 and 3.5,respectively.

$$F_{cs} = \frac{1}{\cos\theta} \tag{3.3}$$

$$F_{tub} = \frac{1}{2} \tag{3.4}$$

$$F_{tlc} = \tan\theta \tag{3.5}$$

where F_{cs} is the compressive force on the diagonal strut, F_{tub} is the tensile force on the upper track and F_{tlc} is the tensile force on the left column.

If the deformed shape is taken into account, the length variation can also be expressed by Equation 3.6.

$$\Delta d = \delta_x \cos\theta - \delta_y \sin\theta \tag{3.6}$$

Addition to Equation 3.6, length variation caused by the compressive force on the diagonal strut F_{cs}, can be stated as Equation 3.7.

$$\Delta d = F_{cs}\frac{d}{E_d t w} = \frac{1}{\cos\theta}\frac{d}{E_d t w} \tag{3.7}$$

where d, E_d, t and w are length, the Young's modulus, thickness and width of the diagonal strut,respectively.

δ_y is the vertical displacement due to lateral unitary load can be expressed as follows:

$$\delta_y = F_{tlc}\frac{d}{E_d t w} \tag{3.8}$$

After combining the Equation 3.6 and 3.8, δ_x can be stated as Equation 3.9.

$$\delta_x = \frac{1}{(\cos\theta)^2}\left(\frac{d}{E_d t w} + \frac{(\sin\theta)^2 h}{E_f A_c}\right) \tag{3.9}$$

By considering the expression of the force F_{tub} that interests the upper track (Equation 3.4), the elongation δ_{p1} substituted in Equation 3.2 can basically be expressed as Equation 3.10.

$$\delta_{p1} = F_{tub}\frac{l/2}{E_d A_b} = \frac{1}{4}\frac{l}{E_f A_b} \tag{3.10}$$

For the equilibrium of the equations on the system, the axial force to the downer track is equal to 1/2, therefore, the elongation of the downer track evaluated in the mid-span δ''_{p1p2} can be stated as Equation 3.11.

$$\delta''_{p1p2} = F_{tdb}\frac{l/2}{E_c A_b} = \frac{1}{4}\frac{l}{E_f A_b} \tag{3.11}$$

Equation 3.12 can be obtained if all equations are considered and substituting in Equation 3.1.

$$\delta_{p1p2} = \frac{1}{(\cos\theta)^2}\left(\frac{d}{E_d t w} + \frac{(\sin\theta)^2 h}{E_c A_c}\right) + 2\frac{1}{4}\frac{l}{E_c A_b} \tag{3.12}$$

In order to get rid of complexity, axial stiffness for each member such as board, track and stud can simply be expressed as follows:

$$k_d = \frac{E_d t w}{d} \tag{3.13}$$

$$k_c = \frac{E_c A_c}{h} \tag{3.14}$$

$$k_b = \frac{E_c A_b}{l} \tag{3.15}$$

If these three equations are substituted in the Equation 3.12, Equation 3.16 can be derived.

$$\delta_{p1p2} = \frac{1}{(\cos\theta)^2}(\frac{1}{k_d} + \frac{(\sin\theta)^2}{k_c}) + \frac{1}{2}\frac{l}{k_b} \tag{3.16}$$

Finally, the stiffness of the frame system D_d can be expressed as follows:

$$D_d = \frac{1}{\delta_{p1p2}} = \frac{k_d(\cos\theta)^2}{1 + \frac{k_d}{k_c}(\sin\theta)^2 + \frac{1}{2}\frac{k_d}{k_b}(\cos\theta)^2} \tag{3.17}$$

3.3. Stiffness Determination of the CFS Panel Due to Experimental Results

The panel parameters can be summarized in the Table 3.1 before evaluations.

Table 3.1. Cross Section Properties of the CFS Panel

$A_b(mm^2)$	169.93
$A_c(mm^2)$	351.36
θ°	63.43
$d(mm)$	2683.28
$h(mm)$	2400
$l(mm^2)$	1200
$E_d(MPa)$	3053
$E_c, E_b(MPa)$	203395
$I_c(mm^4)$	533171.1
$I_b(mm^4)$	267281
$t(mm)$	12.5

where A_b, A_c are the cross sectional area of the track and stud, respectively. is the

angle between stud and downer track, d is the diagonal length of the panel, h and l are the height of the panel and length of the panel, respectively. E_d, E_c, E_b are the Young's modulus of the gypsum wallboard (diagonal strut), stud and track, respectively.

3.3.1. The Panel with 100 and 150 mm screw spacing and 0.9 mm steel thickness

According to the literature it can be concluded that for the elastic deformation 40 percent of the peak load can be taken as elastic load. This deformation value corresponding to this load can be expressed as stiffness of the panel.

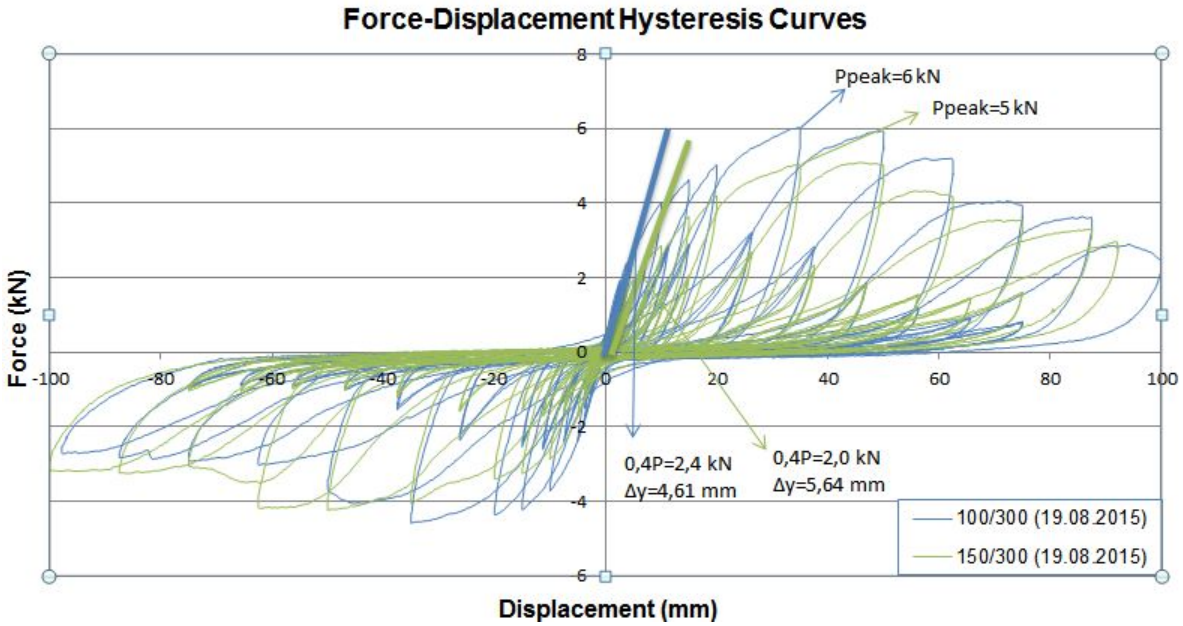

Figure 3.7. Experimental results of the Panel with 100 and 150 mm screw spacing

Rigidity of the panels with 150 mm and 100 mm screw spacing can be expressed as follows:

$$k_{100} = \frac{0.4 * 6.0}{4.61} = 0.52 \ \ kN/mm$$

$$k_{150} = \frac{0.4 * 5.0}{5.64} = 0.35 \ \ kN/mm$$

3.3.2. The Panel with 200 mm screw spacing and 0.9 mm steel thickness

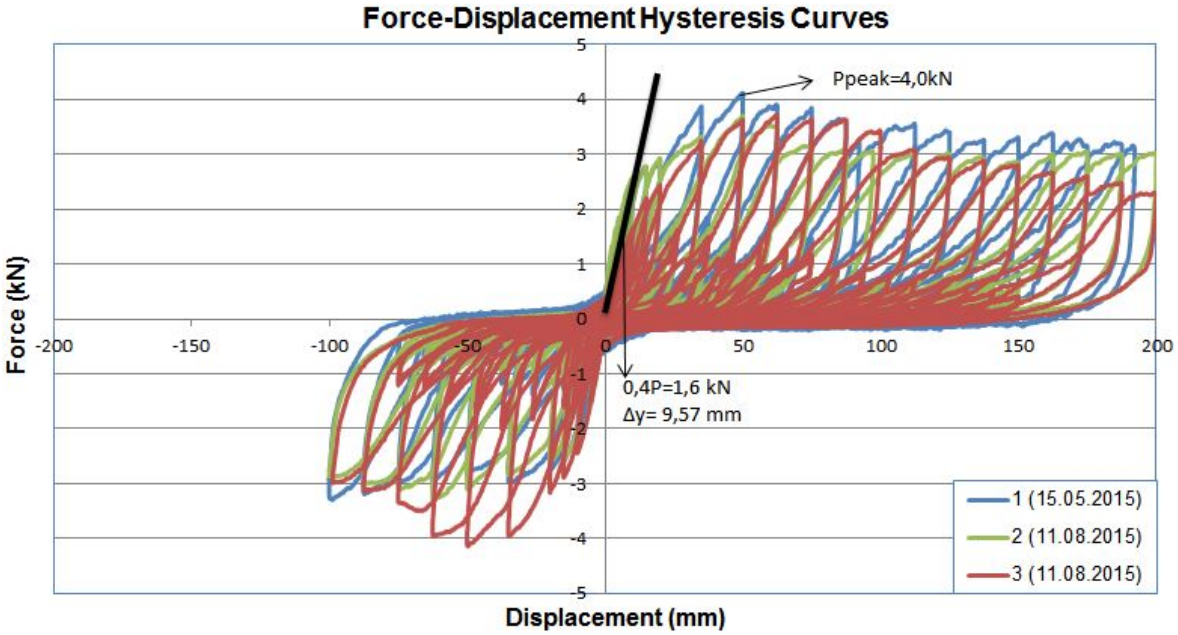

Figure 3.8. Experimental results of the Panel with 200 mm screw spacing

Also, rigidity of the GWB panel with 200 mm screw spacing can be expressed by following equation.

$$k_{200} = \frac{0.4 * 4.0}{9.57} = 0.167 \ \ kN/mm$$

3.3.3. The Panel with 200 mm screw spacing and 1.5 mm steel thickness

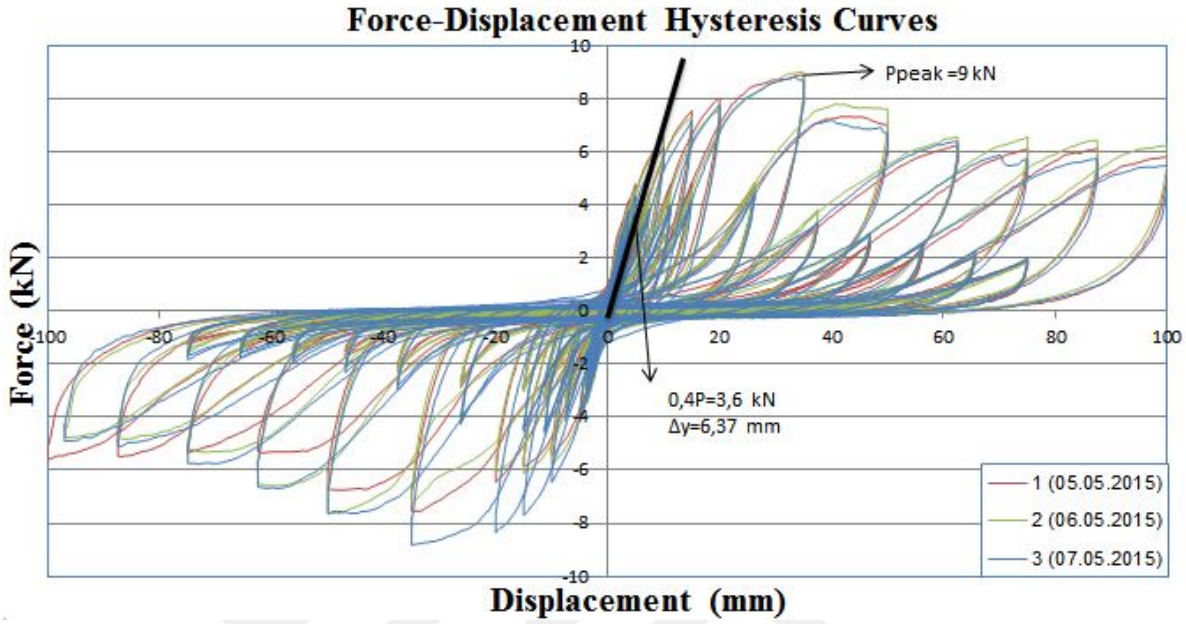

Figure 3.9. Experimental result of the Panel with steel thickness 1.5 mm and 200 mm screw spacing

Rigidity of the GWB panel with 200 mm screw spacing can be expressed by following statement.

$$k_{200} = \frac{0.4 * 9.0}{6.37} = 0.565 \ \ kN/mm$$

3.4. Analytical Investigation of the Panel Stiffness

As can be seen in Figure 3.10, column beam joints are assigned as pinned joint in order to obtain analytical model close to real world structure. Each panel is formed two studs and tracks connected with moment release joints. Due to pinned joints, studs and trucks have no lateral resistance to lateral force. Thus, diagonal element makes the frame system stable and provides lateral rigidity.

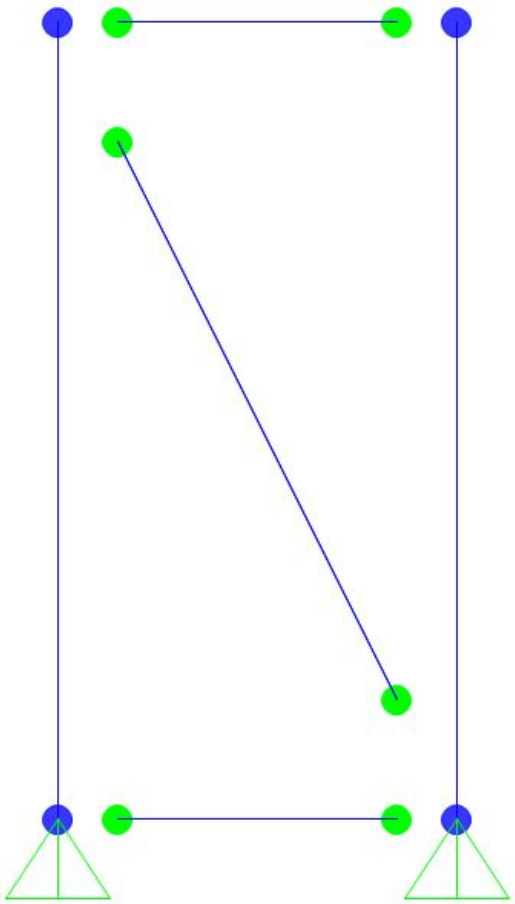

Figure 3.10. Analytical model of the strut model

3.4.1. The Panel with 100/300 screw spacing and 0.9 mm steel thickness

40 percent of lateral peak load obtained from experiments is horizontally applied to the top of the frame. While achieving the lateral displacement obtained from experiment, strut width can be determined.

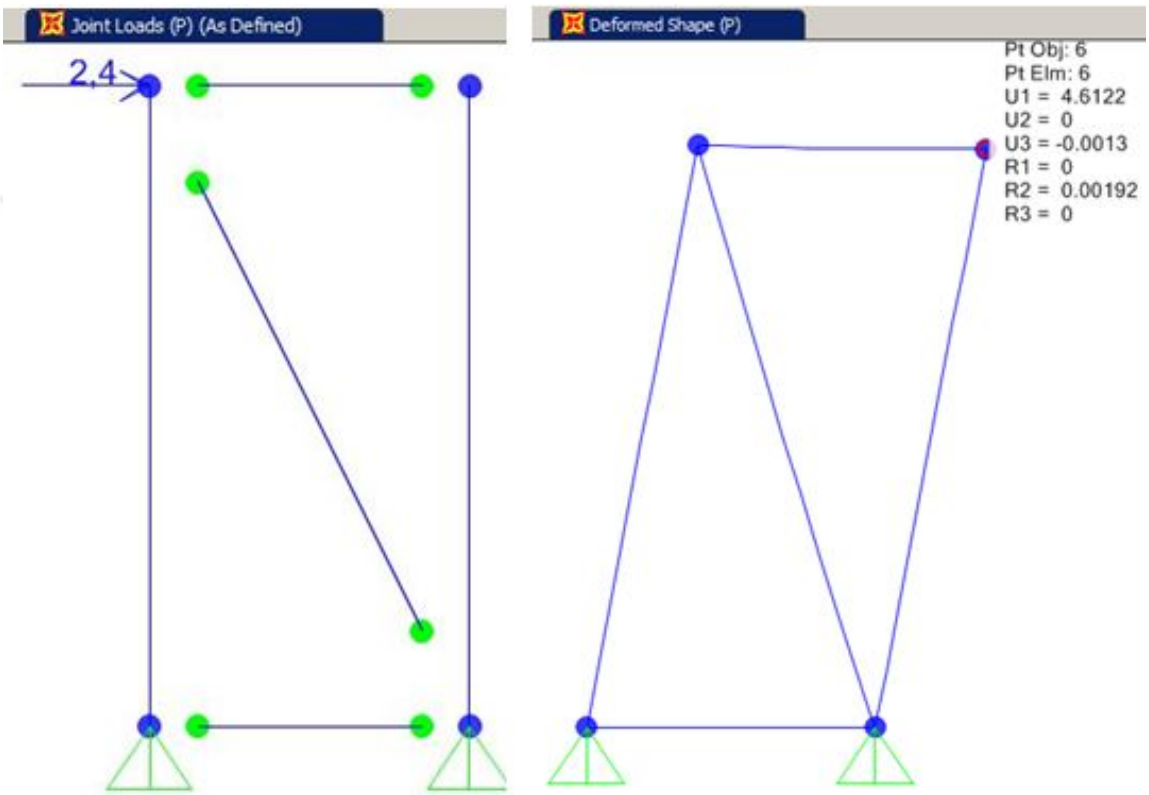

Figure 3.11. Lateral load and displacement values

After applying 2.4 kN lateral force to the top of the panel, the lateral displacement was reached 4.61 mm as shown in the Figure 3.11 In order to achieve the same results with experiments, the strut width w is considered as 196.5 mm by trial and error method.

Full frame lateral stiffness can be expressed by Equation 3.18 according to Asteris *et al.* [26].

$$D_i = D_d + D_f \tag{3.18}$$

where D_i is the lateral stiffness of the simplified model, D_d is the lateral stiffness due to diagonal strut and D_f is the lateral stiffness due to steel frame. However, pinned joints cannot allow the lateral resistance, thus, D_f could be taken "0" (zero). Therefore, D_i equals to D_d which is expressed in Section 3.3 Equation 3.16.

In order to be proved the close match between the test result and analytical evaluations, model the stiffness and displacement calculations of the strut model corresponding to the panel with 100/300 screw spacing are given in detail as follows.

$$k_d = \frac{3053 * 12.5 * 196.5}{2683.28} = 2.79 \ \ kN/mm$$

$$k_c = \frac{3053 * 12.5 * 196.5}{2683.28} = 29.78 \ \ kN/mm$$

$$k_b = \frac{3053 * 12.5 * 196.5}{2683.28} = 28.80 \ \ kN/mm$$

Thus, lateral stiffness can be evaluated by following expression.

$$D_d = \frac{2.79(\cos 63.43)^2}{1 + \frac{2.79}{29.78}(\sin 63.43)^2 + \frac{2.79}{28.80}(\cos 63.43)^2}$$

$$D_d = 0.515 \ \ kN/mm$$

δ_x generic displacement of the simplified model and the lateral displacement Δ_x can be evaluated by Equation 3.9.

$$\delta_x = 0.0019$$

$$\Delta_x = 0.0019 * 2400 = 4.61 \ \ mm$$

The calculations will be summarized and the results will be compared by strut models during following sections.

3.4.2. The Panel with 150/300 screw spacing and 0.9 mm steel thickness

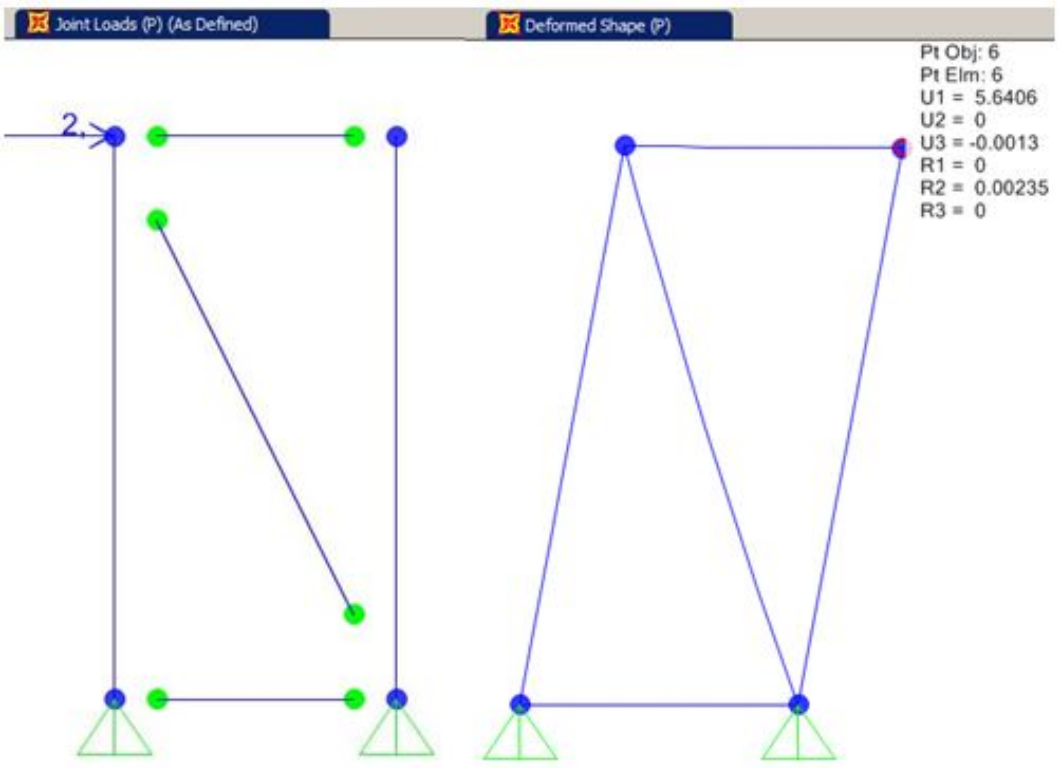

Figure 3.12. Lateral load and displacement values

$$k_d = 1.86 \ \ kN/mm$$

$$k_c = 29.78 \ \ kN/mm$$

$$k_b = 28.80 \ \ kN/mm$$

$$D_d = 0.35 \ \ kN/mm$$

$$w = 130.8 \ \ mm$$

$$\delta_x = 0.0019$$

$$\Delta_x = 0.00282122 * 2000 = 5.64 \ \ mm$$

3.4.3. The Panel with 200/300 screw spacing and 0.9 mm steel thickness

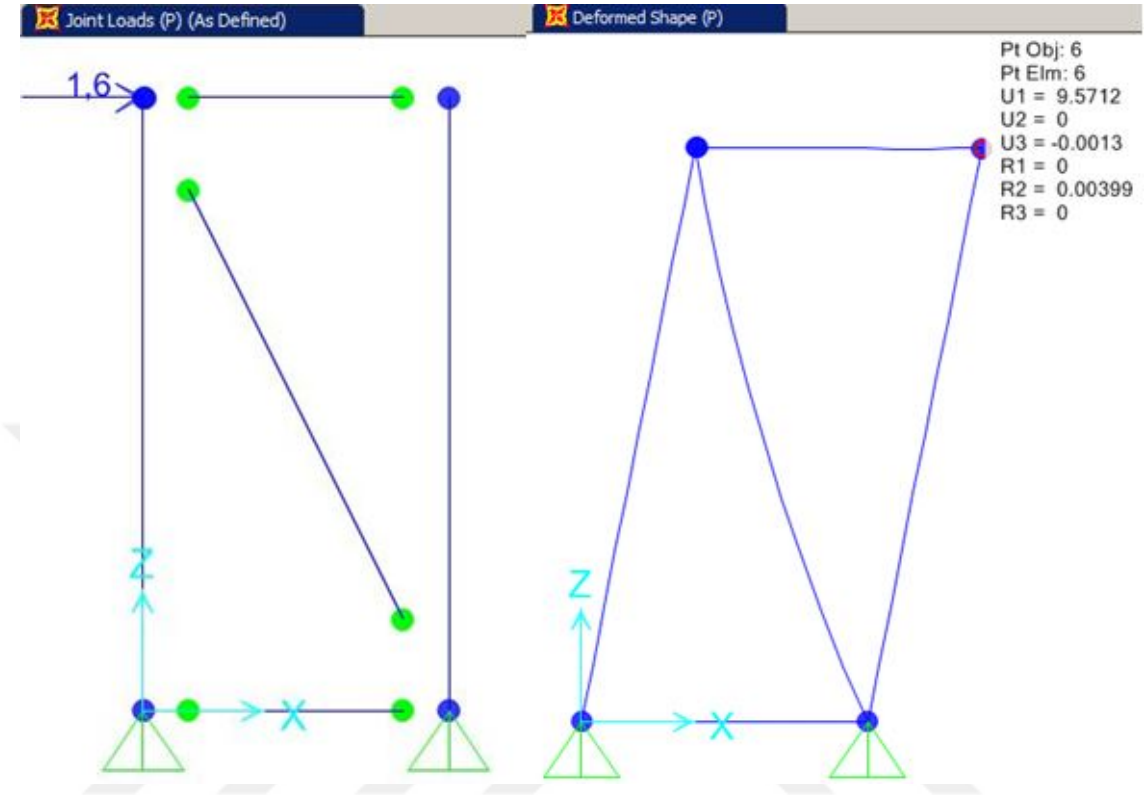

Figure 3.13. Experimental results of the Panel with 200 mm screw spacing

$$k_d = 0.855 \ \ kN/mm$$

$$k_c = 29.78 \ \ kN/mm$$

$$k_b = 28.80 \ \ kN/mm$$

$$D_d = 0.1667 \ \ kN/mm$$

$$w = 60.1 \ mm$$

$$\delta_x = 0.005982$$

$$\Delta_x = 0.005982 * 1660 = 9.57 \ mm$$

3.4.4. The Panel with 200/300 screw spacing and 1.5 mm steel thickness

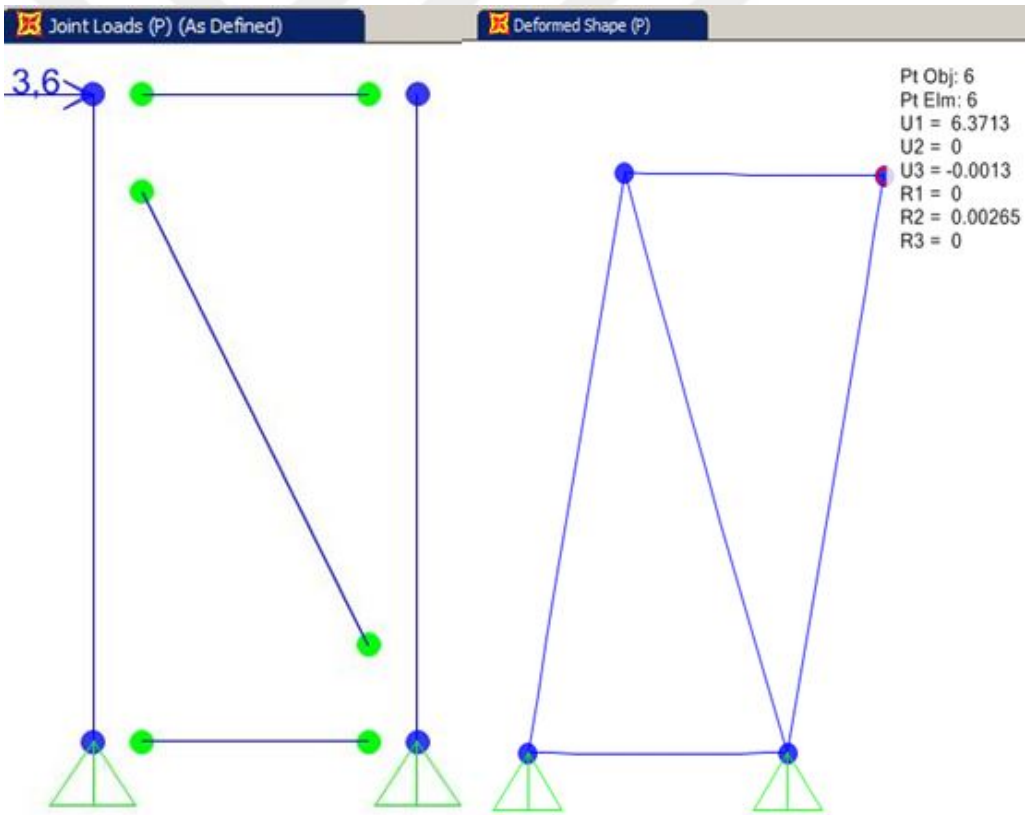

Figure 3.14. Lateral load and displacement values

$$k_d = 2.958 \ kN/mm$$

$$k_c = 49.628 \ \ kN/mm$$

$$k_b = 47.683 \ \ kN/mm$$

$$D_d = 0.5616 \ \ kN/mm$$

$$w = 208.9 \ \ mm$$

$$\delta_x = 0.00176$$

$$\Delta_x = 0.00176x3600 = 9.57 \ \ mm$$

3.5. Comparision of the Experimental and Analytical Results in terms of Lateral Stiffness

Table 3.2. . Comparision of the experimental and analytical results

Steel thickness (mm)	**Screw spacing (ext/int)**	**0.4 P (kN)**	**Displacement x-dir (mm)**	**Stiffness (experimental) (kN/mm)**	**Stiffness (analytical) (kN/mm)**
0.9	100/300	2.4	4.61	0.52	0.515
0.9	150/300	2.0	5.64	0.355	0.352
0.9	200/300	1.6	9.57	0.167	0.167
1.5	200/300	3.6	6.37	0.565	0.562

3.6. The Equivalent Strut Width Proposal

Firstly,this formula has only been proposed in the context of the thesis, this formula needs to be studied and developed further so that it can be used in the design of real-world building.

The strut width is proposed by comparing rigidity obtained from experiments and equivalent strut models. The strut width essentially depends on steel thickness, aspect ratio, diagonal length and screw spacing. As can be understood from the results of the experiment, screw spacing plays directly an important role in lateral stiffness. The recommended equivalent strut width is as follows:

$$w = 25000\frac{t_s^2}{s} \tag{3.19}$$

where, w is the suggested strut width (mm), t_s is steel thickness (mm), s is exterior screw spacing (mm).

The most important parameters affecting strut width were taken into consideration while obtaining the formula. While steel thickness t_s increases, lateral stiffness

increases; on the contrary, screw spacing increases, lateral stiffness decreases. Thus, increasing in steel thickness and decreasing in screw spacing increase the width of the equivalent strut thickness. While the strut width equation derived mentioned in above, it was fully empirically obtained by trial and error solution.

According to the parameters given in Table 3.1, the steel thickness is 0.9 mm and screw spacing is 200 mm, the strut width of a panel will be as follows:

$$w = 25000\frac{0.9^2}{200}$$

$$w = \mathbf{101.25}\ mm$$

The equivalent strut width will be used in Section 4 in order to analyze the one story structure.

4. ANALYTICAL STUDY OF A TYPICAL ONE-STORY CFS STRUCTURE CREATED WITH DIAGONAL STRUTS

4.1. Introduction

In this section, seismic performance assessment is performed using the equivalent diagonal strut obtained in the previous sections. The width of the strut is 101.25 mm, which corresponds to 200 mm screw spacing. This analytical study is presented as a result of the studies in Section 3 and detailed with cross-section calculations. The ultimate purpose of this application is to ensure the capability of cold-formed steel structures to possess a reasonable performance in seismic inclined regions such as Turkey.

4.2. Properties of the Structure

The single-story cold formed steel building to be examined is selected as an architectural project that can meet the needs. All measurements can be seen in Figure 4.1

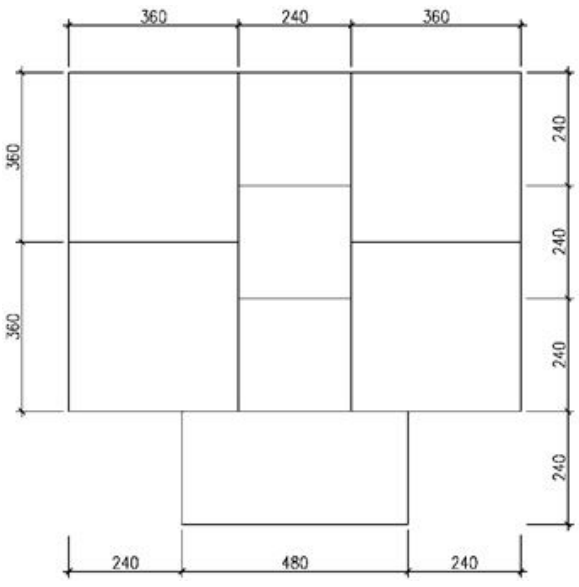

Figure 4.1. Plan view of the structure

In order to illustrate this structure and to see diagonal struts more clearly, the extruded view of the structure was shown in Figure 4.2

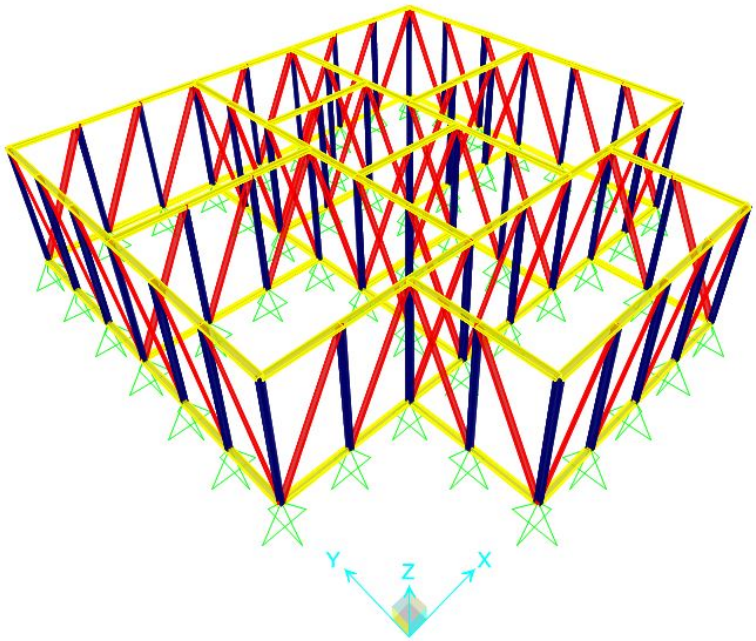

Figure 4.2. Extruded-3D View of the Structure

Panel was represented by two studs, two tracks and one equivalent strut. The height and length of the panel are 2.4 m and 1.2 m, respectively. The material parameters were obtained from the manufacturer and used in these experiments are shown in Table 4.1

Table 4.1. Mechanical properties of gypsum wallboard and CFS

Properties	**Modulus of Elasticity, E(MPa)**	**Weight per unit Volume(kg/m^2)**	**Poisson's Ratio**
Gypsum Wallboard	3053 in short direction 2404 in long direction	640	0.167
CFS	203395	7849	0.3

4.3. Loads Assigned to the Structure

4.3.1. Dead, Live and Snow Loads

Firstly, the floor weight on the structure is considered as composite floor and roughly 25 kN/m^2. Floor thickness is 0.2 meter, so the dead load from here is taken as 5 kN/m^2. This load is distributed to the corresponding Area and assigned to the upper tracks as a load in the gravity direction; in addition, since this structure represents a CFS with panel, the actual panel weight is taken into account the weight of the equivalent strut panel and loaded into the structure. According to the calculation practices and the roof coatings used in the market, the roof dead load was taken as 105 kg/m^2 and snow load was taken as 75 kg/m^2.

All these loads were taken and multiplied by the effective areas and loaded to the related tracks in the direction of gravity. After all these load assignments, the weight of the structure can be seen in Table 4.2

Table 4.2. Weight of the structure

Output Case	**Case Type**	**Global FX**	**Global FY**	**Global FZ**
Text	Text	kN	kN	kN
G+0.3Q	Combination	8,535E-14	5.133	525.295

4.3.2. Earthquake Loads

The structure was selected as Tuzla district of Istanbul, which is an earthquake prone area, and Ground type B class was accepted as ground condition. During the calculation of the earthquake, TEC 2018 [5] section 2 and Section 10, which are related to light steel structures, were taken into consideration. Moreover, to obtain parameters such as S_s and S_1 https://tdth.afad.gov.tr/TDTH/main.xhtml values are taken from the named site. Here S_s is the map spectral acceleration coefficient for the short

period region and S_1 is the map spectral acceleration coefficient for the 1.0 second period. Earthquake level is designated as DD-2 Earthquake Earth Motion which characterizes the earthquake ground motion where the probability of exceeding the spectral magnitudes by 50 years is %10 and the corresponding repetition period is 475 years.

$$S_{DS} = S_S.F_S \tag{4.1}$$

$$S_{D1} = S_1.\gamma_F.F_1 \tag{4.2}$$

F_S and F_1 are local ground coefficients and obtained from TEC2018 section 2. γ_F is the coefficient of susceptibility to fault and 1.0 can be taken for this structure. S_{DS} ve S_{D1} are design spectral acceleration coefficients can be calculated with Equation 4.1 and 4.2. The earthquake parameters to be used were summarized in the table below.

Table 4.3. Earthquake Parameters

S_S	14.147
F_S	0.9
S_{DS}	1.0323
S_1	0.319
F_1	0.8
S_{D1}	0.25527
γ_F	1.0

Horizontal design spectrum corner periods T_A and T_B can be calculated according to the following equations.

$$T_A = 0.2\frac{S_{D1}}{S_{DS}}; \qquad T_B = \frac{S_{D1}}{S_{DS}} \tag{4.3}$$

Thus, by substituting the value of S_{DS} and S_{D1} into the Equation 4.3, the corner periods can be found as follows:

$$T_A = 0.049 \ \ sec; \qquad T_B = 0.247 \ \ sec$$

In Chapter 10 of the TEC2018, it has been stated that the natural vibration time should be taken $T = 0.2$ sec to calculate earthquake loadings. Therefore, the horizontal elastic design spectral accelerations of $S_{ae}(T)$ have been defined in the earthquake regulation according to the natural vibration period and the value in terms of gravitational acceleration $[g]$.

$$S_{ae}(T) = S_{DS} \quad (T_A \leq T \leq T_B) \tag{4.4}$$

$$S_{ae}(T) = 1.0323 \ \ g$$

$S_{ae}(T)$ vertical and horizontal elastic spectral accelerations in the same section, depending on the natural vibration period in terms of gravitational acceleration $[g]$ can be stated as follows.

$$S_{aeD}(T) = 0.8 S_{DS} \frac{T_{BD}}{T} \quad (T_{BD} \leq T \leq T_{LD}) \tag{4.5}$$

$$S_{aeD}(T) = 0.339 \ \ g$$

Load-bearing system behavior coefficient R and overstrength coefficient D were selected from Table 4.1 of TEC 2018 [5], 3 and 2, respectively. Thus, earthquake reduction factor can be found as follows:

$$R_a(T) = D + (\frac{R}{I} - D)\frac{T}{T_B} \quad (T \leq T_B) \tag{4.6}$$

$$R_a(T) = 2.75$$

Thus, the total base shear force given in the specification can be obtained from the Equation 4.7

$$V_{tE}^{(x)} = m_t \, S_{aR}(T_p^{(x)}) \geq 0.04 \, m_t \, I \, S_{DS} \, g \tag{4.7}$$

$$V_{tE}^{(x)} = 171.8 \;\; kN$$

X-direction total base shear force obtained from analytical model can be seen in Table 4.4

Table 4.4. Total base shear force

Output Case	**Case Type**	**Step Type**	**Global FX**
Text	Text	Text	kN
SpecX	LinRespSpec	Max	171,8

4.4. Load Combinations

The following load combinations including earthquake effects were taken as the basis for the design of the structural system elements. Since the design approach was applied from according to load strength coefficients method, Dead Load was taken as 1.2G instead of 1.0G as in the specification.

$$1.2G + Q + 0.2S \pm E_{dx} \pm 0.3E_{dy} + 0.3E_{dz} \tag{4.8}$$

where G is the structure dead load Q is the moving load Edx and Edy is the horizontal earthquake components Edz is the vertical earthquake force.

4.5. Demands of the Structure

4.5.1. Shear Demand

After performing the SAP2000 [6] analysis, the shear demand from each section can be found by dividing the total base shear obtained by the number of studs available.

$$shear\ demand = Total\ base\ shear\ force\ /\ total\ \ number\ \ of\ panels$$

$$shear\ demand = 171\ \ kN\ /\ 58\ frames = \mathbf{2.95\ \ kN}$$

4.5.2. Axial Demand

When the load combinations were assigned and analyzed, the maximum axial load to the cross-sections can be found by SAP2000 [6] program. Maximum axial load can be visualized by the Table 4.5

Table 4.5. Maximum Axial Force

Frame	Station	OutputCase	CaseType	StepType	P
Text	mm	Text	Text	Text	kN
13	0	1.2G+Q+0.2S+EdH2+0.3EdZ	Combo	Min	-30.15
13	0	1.2G+Q+0.2S+EdH3+0.3EdZ	Combo	Min	-30.15
13	0	1.2G+Q+0.2S+EdH4+0.3EdZ	Combo	Min	-30.15

Furthermore, the maximum axial load to the element in the SAP2000 [6] model was shown in the figure below.

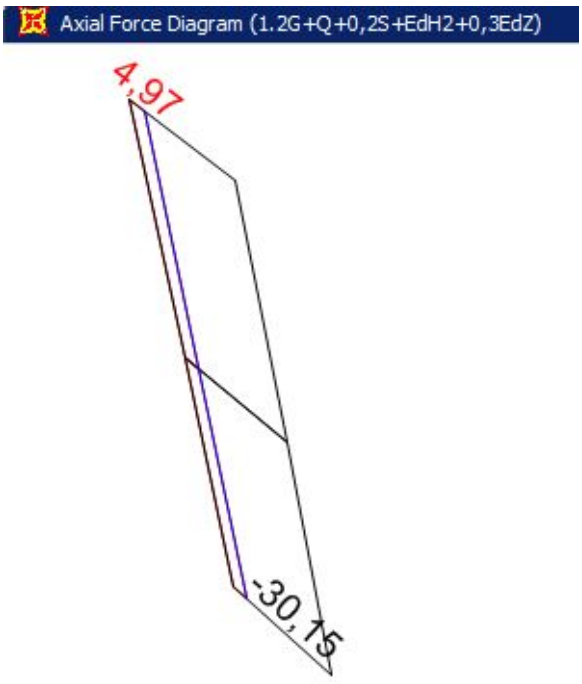

Figure 4.3. Maximum Axial Force (kN)

4.6. Capacity Calculations

Four main capacity calculations should be taken into account and these are:

- Column buckling of the studs between fasteners,
- Flexural – torsional column buckling,
- Local and distortional buckling,
- Capacity check of panel,

Frame elements of the structure must be avoided from these four failure modes for a safe and stiff structure. While column buckling of the studs between fasteners and flexural – torsional column buckling are occured due to axial load, shear failure of the sheathing could be presented due to shear load. These failure modes were investigated in this section, respectively.

4.6.1. Section Properties

The stud element selected in the example was the double C profile section selected in the experiments. Thus, the same cross section was performed in the analytical investigations and properties given by the Table 4.6. All dimensions are in millimeters in the Figure 4.4.

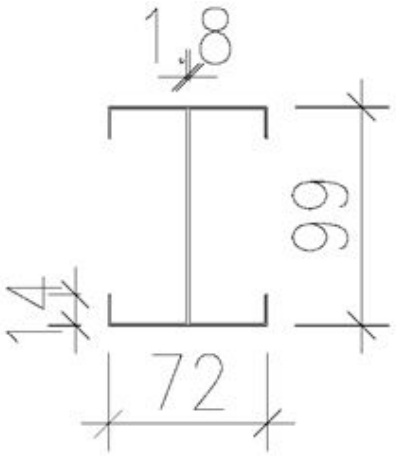

Figure 4.4. Dimensions of the double C cross section

Table 4.6. Section Properties

Cross Section Area	$A_g(mm^2)$	351.36
Moment of Inertia (x)	$I_x(mm^4)$	533171.1
Moment of Inertia (y)	$I_y(mm^4)$	115183.6
Center of Gravity about y	$C_0G_y(mm)$	0
Radius of Gyration (x)	$r_x(mm)$	38.9545
Radius of Gyration (y)	$r_y(mm)$	18.1059
St. Vennant Torsional Constant	$J(mm^4)$	238.8694
Shear Center	$e(mm)$	0
Warping Constant	$C_w(mm^6)$	205954535
Elastic Modulus	$E(MPa)$	203395
Shear Modulus	$G(MPa)$	78228.98
Shear Center to Centroid Along (x)	$x_0(mm)$	0
Shear Center to Centroid Along (y)	$y_0(mm)$	0
Polar Radius of Gyration	$r_0(mm)$	42.9566
Yield stress of steel	$F_y(MPa)$	227.5

4.6.2. Nominal Buckling Stress for Column Buckling of Stud between Fasteners (Elastic Flexural Buckling)

Since screw spacing was selected as 200/300 mm, exterior spacing was included the evaluations as 200 mm.

$$KL = 2 * spacing\ of\ screw \tag{4.9}$$

$$KL = 2 * 200 \ = \ 400 \ mm$$

Slenderness ratio, KL/r can be computed for both x and y axis, then Euler Buckling Stress would be obtained as follows:

$$F_e = \frac{\pi^2 E}{(\frac{KL}{r})^2} \tag{4.10}$$

Then λ_c should be computed by the given Equation 4.11.

$$\lambda_c = \sqrt{\frac{F_y}{F_e}} \tag{4.11}$$

In case λ_c smaller than 1.5, Equation 4.12 can be used for nominal buckling stress.

$$F_n = (0.658^{\lambda_c^2})F_y \tag{4.12}$$

For x axis:

$$\frac{KL}{r} = \frac{400}{38.9545} = 10.268$$

$$F_e = \frac{\pi^2 203395}{(10.268)^2} = 19040.06 \ \ MPa$$

$$\lambda_c = \sqrt{\frac{227.5}{19040.06}} = 0.109 < 1.5$$

$$F_n = (0.658^{0.109^2})227.5 = \mathbf{226.37 \ \ MPa}$$

For y axis:

$$\frac{KL}{r} = \frac{400}{18.059} = 22.15$$

$$F_e = \frac{\pi^2 203395}{(22.15)^2} = 4075.02 \ MPa$$

$$\lambda_c = \sqrt{\frac{227.5}{4075.02}} = 0.236 < 1.5$$

$$F_n = (0.658^{0.236^2})227.5 = \mathbf{222.25\ MPa}$$

4.6.3. Elastic Torsional Buckling

Euler buckling stress for elastic torsional buckling can be obtained as follows:

$$F_e = \frac{1}{2\beta}[(\sigma_{ex} + \sigma_t) - \sqrt{(\sigma_{ex} + \sigma_t)^2 - 4\beta\sigma_{ex}\sigma_t} \tag{4.13}$$

where:

$$\beta = 1 - (\frac{x_0}{r_0})^2 \tag{4.14}$$

$$\sigma_{ex} = \frac{\pi^2 E}{(\frac{KL}{r_x})^2} \tag{4.15}$$

$$\sigma_t = \frac{1}{Ar_0^2}[GJ + \frac{\pi^2 EC_w}{(KL)^2}] \tag{4.16}$$

$$\beta = 1 - (\frac{0}{42.9566})^2 = 1$$

$$\sigma_{ex} = 19038.65 \ MPa$$

$$\sigma_t = F_e = 1249.395 \ MPa$$

$$\lambda_c = \sqrt{\frac{227.5}{1249.395}} = 0.426 < 1.5$$

$$F_n = (0.658^{0.426^2})227.5 = \mathbf{210.82 \ MPa}$$

4.6.4. Nominal Buckling Stress for Overall Column Buckling

To prevent flexural and/or torsional overall column buckling, F_n should be calculated by using smaller one of two σ_{CR} values for double C-sections.

$$\sigma_{CR1} = \sigma_{ey} + \bar{Q}_a \tag{4.17}$$

where:

$$\sigma_{ey} = \frac{\pi^2 E}{(\frac{KL}{r_y})^2} \tag{4.18}$$

$$\bar{Q}_a = \frac{\bar{Q}}{A} \tag{4.19}$$

$$\bar{Q} = \bar{Q}_0(2 - \frac{s}{s'}) \tag{4.20}$$

The sheathing parameters were taken from AISI [4] Specification and the related table can be seen Figure 4.5.

Table D4 Sheathing Parameters[1]

Sheathing(2)	$\bar{Q}_o$ k	$\bar{Q}_o$ kN	$\bar{\gamma}$ length/length
3/8 in. (9.5 mm) to 5/8 in. (15.9 mm) thick gypsum	24.0	107.0	0.008
Lignocellulosic board	12.0	53.4	0.009
Fiberboard (regular or impregnated)	7.2	32.0	0.007
Fiberboard (heavy impregnated)	14.4	64.1	0.010

Figure 4.5. Sheathing Parameters

$$\sigma_{ey} = \frac{\pi^2 203395}{(\frac{2400}{18.1059})^2} = 114.25 \ \ MPa$$

$$\bar{Q} = 107000(2 - \frac{200}{305}) = 143836.07 \ \ N$$

$$\bar{Q}_a = \frac{143.836}{351.36} = 409.36 \ \ MPa$$

$$\sigma_{CR1} = 114.25 + 409.36 = \mathbf{523.62} \ \ MPa$$

4.6.5. Torsional-Flexural Overall Column Buckling

$$\sigma_{CR2} = \frac{1}{2\beta}[(\sigma_{ex} + \sigma_{tQ}) - \sqrt{(\sigma_{ex} + \sigma_{tQ})^2 - 4\beta\sigma_{ex}\sigma_{tQ}} \tag{4.21}$$

where:

$$\bar{Q}_t = \frac{\bar{Q}d^2}{4Ar_0^2} \tag{4.22}$$

$$\sigma_{tQ} = \sigma_t + \bar{Q}_t \tag{4.23}$$

$$\sigma_{ex} = \frac{\pi^2 203395}{(\frac{2400}{38.9545})^2} = 528.85 \ \ MPa$$

$$\sigma_t = 139.53 \ \ MPa$$

$$\bar{Q}_t = 404.37 \ \ MPa$$

$$\sigma_{tQ} = 543.9 \ \ MPa$$

$$\sigma_{CR2} = \mathbf{528.85 \ \ MPa}$$

Therefore, 528.85 MPa governs for overall column buckling.

$$\lambda_c = \sqrt{\frac{227.5}{528.85}} = 0.656 < 1.5$$

$$F_n = (0.658^{0.656^2})227.5 = \mathbf{190.01\ MPa}$$

4.6.6. Local Buckling

Local buckling can be examined for web, flange and lip and the element approach which is classical solution for prediction of local buckling according to Schafer *et al.*, (2002) [28].

web local buckling:

$$\sigma_{Crl} = k\frac{\pi^2 E}{12(1-\upsilon^2)}(\frac{t}{h})^2 \qquad k = 4 \tag{4.24}$$

flange local buckling:

$$\sigma_{Crl} = k\frac{\pi^2 E}{12(1-\upsilon^2)}(\frac{t}{b})^2 \qquad k = 4 \tag{4.25}$$

lip local buckling:

$$\sigma_{Crl} = k\frac{\pi^2 E}{12(1-\upsilon^2)}(\frac{t}{d})^2 \qquad k = 0.43 \tag{4.26}$$

where is Poisson's ratio, t is thickness, b flange width and d is the depth of the lip. Furthermore, k values are a kind of constant and have been proposed by Schafer *et al.*, (2002). The critical elastic local column buckling can be chosen minimum of these there stresses.

$$\sigma_{Crl} = 114.89\ \ MPa$$

According to AISI [4] specification local buckling can be calculated as follows.

$$F_n = 190.01 \ \ MPa$$

$$\lambda_c = \sqrt{\frac{190.01}{114.89}} = 1.29 > 0.776$$

$$F_{nl} = [1 - 0.15(\frac{\sigma_{Crl}}{F_n})^{0.4}](\frac{\sigma_{Crl}}{F_n})^{0.4} F_n \tag{4.27}$$

$$F_{nl} = \mathbf{136.32 \ MPa}$$

4.6.7. Distortional Buckling

As the stud is covered on both sides, it was not expected to occur any distortional buckling. As can be seen from the experiment, all types of failure was shear failure and occurred at sheathing to stud fastener. However, distortional buckling can be checked to not to face any negative situation and can be found as follows according to Schafer *et al.*, (2002) [28].

$$F_{db} = \frac{k_{\phi fe} + k_{\phi we}}{k_{\phi fg} + k_{\phi wg}} \tag{4.28}$$

where $k_{\phi fe}$ is elastic rotational spring stiffness of the flange and should be calculated as follows:

$$k_{\phi fe} = (\frac{\pi}{4})^4 [EI_x(x_0 - h_x)^2 + EC_w - E\frac{I_{xy}}{I_y}(x_0 - h_x)^2] + (\frac{\pi}{L})^2 GJ \tag{4.29}$$

$k_{\phi fg}$ is geometric rotational stiffness of the flange and should be found by the following equation:

$$k_{\phi fg} = (\frac{\pi}{L})^2[A[(x_0 - h_x)^2(\frac{I_{xy}}{I_y}) - 2y_0(x_0 - h_x)(\frac{I_{xy}}{I_y}) + h_x^2 + y_0^2] + I_x + I_y] \quad (4.30)$$

Also $k_{\phi we}$ and $k_{\phi wg}$are elastic and rotational stiffness of the web, respectively and can be found by following equations.

$$k_{\phi we} = \frac{t^3 E}{6h(1 - \upsilon^2)} \quad (4.31)$$

$$k_{\phi wg} = (\frac{\pi}{L})\frac{th^3}{60} \quad (4.32)$$

After all calculations were operated, the distortional buckling can be obtained as follows:

$$F_{db} = \mathbf{643.14\ MPa}$$

4.6.8. Axial Capacity

By comparing all nominal buckling stresses, the smallest one which is 183.9 MPa is chosen. Then, to obtain allowable axial load, the effective area needs to be found. Although different approaches are available, the method based on a multiplier is chosen for this example and taken 0.85.

$$A_e = 0.85A_g = 0.85 * 351.36 = 298.66\ \ mm^2 \quad (4.33)$$

$$P_n = F_n A_e = 136.32 * 298.66 * 10^{-3} = 40.71 \ kN \tag{4.34}$$

$$P_u = \phi_c P_n = 0.85 * 40.71 = \mathbf{34.6 \ kN} \tag{4.35}$$

$$30.15 \ kN < 34.6 \ kN \ OK! \ Axial \ Demand < Axial \ Capacity$$

4.6.9. Shear Capacity

In order to obtain shear capacity, earthquake code is utilized. The characteristic strength per meter of the sheathing material is taken as 2.7 kN/m. In the code, it is said that that the values obtained by the experiments done in the laboratory can be used as characteristic strength of sheathing that's why we used the value of 2.7*1.5 = 4.05 kN/m as characteristic strength of sheathing. Also, ϕ value is obtained as 0.65.

$$V_c = \phi * v_c * \Sigma L_i \tag{4.36}$$

$$V_c = 0.65 * 4.05 * 1.2 = 3.16 \ kN \ per \ panel$$

Since the panel has two-sided boards, this value is multiplied by 2 for load per frame.

$$V_c = 0.65 * 4.05 * 1.2 * 2 = \mathbf{6.32 \ kN} \ per \ panel$$

Although we calculated shear capacity, it is not as important as first two, since it depends on sheathings and sheathings can be replaced easily if any failure occurs.

$$2.95 \ kN < 6.32 \ kN \ OK! \ Shear \ Demand < Shear \ Capacity$$

5. CONCLUSIONS AND FUTURE WORKS

In this section, the main conclusions drawn from this study and the questions that come to mind during these studies are stated under the future works section. Conclusions of this study and future works can guide researchers in future studies. Cold formed steel structures still contain many unknowns that require study on. The capacity of the structure depends on board type, board thickness, screw type, screw spacing, anchorage type, anchorage spacing, steel thickness, and section properties of steel members. Research for this type of structure, which contains many unknown factors, is increasing day by day. Both previous experiments and equivalent strut study are also the product of this curiosity.

5.1. List of Conclusions

- In order to determine the lateral stiffness of the panels, a series of experiments were conducted in Structures Laboratory of Boğaziçi University and this was the inspiration for the thesis. Force-displacement values obtained from these experiments were used in this study. The lateral stiffness of the CFS panel was determined by stated equations.
- While engineers can easily access parameters such as steel thickness, sheathing type, aspect ratio, screw spacing causes complexity in calculations. In order to model the structure correctly, screws must be defined as link elements, which is a very difficult and complex process. Equivalent strut model was proposed instead of modeling screws for both prediction and ease of calculations.
- Equivalent strut width was formulated by making comparison between analytical and experimental results.
- This formula has only been proposed for this study, and the formula needs to be studied and developed.
- A one story structure building which is assigned to equivalent strut was analyzed and earthquake performance was investigated. As a result, after analytical study of the typical one story structure was completed, the performance check of the

structure has been carried out with respect to the base shear and axial force analysis. The demand for the structure to be compared with the capacity is obtained from the design spectrum of the Turkish Earthquake Code. The results of the comparison of capacity and demand showed that such structures with the equivalent strut obtained with this formula can be a reliable structure.

5.2. Future Works

- This Equivalent strut width formula has only been proposed for this study, and the formula needs to be studied and developed.
- As a future work, the formula can be improved by conducting more experiments.
- A new equivalent strut model can be proposed by changing the aspect ratio or performing experiments with the panel with opening.
- The performance assessment can be done for multi-story building by using the proposed formula in this thesis.
- The diagonal strut models with different 2 strut or 3 strut models in the literature or the strut model with eccentricity can be investigated for these types of structures.
- The formula can be further improved by experiments using different steel thicknesses and using different sheathing types.

REFERENCES

1. Dubina, D., V. Ungureanu and R. Landolfo, *Design of Cold-Formed Steel Structures*, Wilhelm Ernst & Sohn Verlag, Berlin, 2012.

2. "Cold-Formed Steel Framed House", `https://www.wzhhouse.com/Case-Show/Cold-formed-Steel-Frame-House-10.html`.

3. "A CFS structure made with modular system", `http://www.containex.ba/hr/referentni-projekti/hu/mobilna-cvjecarnica-netta-hu-nagykanizsa`.

4. American Iron and Steel Institute-S213-07, "North American Standard for Cold-Formed Steel Framing-Lateral Provisions", 2007, washington, D.C. *American Iron and Steel Institute*-S213-07.

5. Turkish Earthquake Code, *"Specification of Building and Earthquake to be built in Turkey"*, *Presidency of emergency and disaster*, Ankara, 2018.

6. Computers and Structures Incorporated SAP2000 v17, 2015, "Integrated Finite Element Analysis and Design of Structures", *Computers and Structures Incorporated, Berkeley*, California, USA.

7. American Society for Testing and Materials E2126, 2011, "Standard Test Methods for Cyclic (Reversed) Load Test for Shear Resistance Vertical Elements of the Lateral Force Resisting Systems for Buildings", *American Society for Testing and materials International, West Conshohocken*, PA, 2006, DOI: 10.1520/E2126-11, *www.astm.org*.

8. Miller, T. H. and T. Pekoz, "Behavior of cold-formed steel wall stud assemblies", *Journal of Structural Engineering*, Vol. 119, No. 2, pp. 641–651, 1993.

9. Miller, T. H. and T. Pekoz, "Behaviour of gypsum-sheathed cold-formed steel wall

studs", *Journal of Structural Engineering*, Vol. 120, No. 5, pp. 1644–1650, 1994.

10. Serette, R. L. and K. Ogunfunmi, "Shear Resistance of Gypsum-Sheathed Light-Gauge Steel Stud Walls", *Journal of Structural Engineering*, Vol. 122, No. 4, pp. 383–389, 1996.

11. Serrette, R. L., J. Encalada, M. Juadines and H. Nguyen, "Static Racking Behavior of Plywood, OSB, Gypsum and Fiberbond Walls with Metal Framing", *Journal of Structural Engineering*, Vol. 123, No. 8, pp. 1079–1086, 1997.

12. Rogers, C. A., A. E. Branston, F. A. Boudreault and C. Y. Chen, "Steel Frame / Wood Panel Shear Walls: Preliminary Design Information For Use With The 2005 NBCC", *13th World Conferance on Eartquake Engineering*, No:1999.

13. Fülöp, L. A. and D. Dubina, "Performance of wall-stud cold-formed shear panels under monotonic and cyclic loading Part I: Experimental research", *Thin-Walled Structures*, Vol. 42, pp. 321–338, 2004.

14. Fülöp, L. A. and D. Dubina, "Performance of wall-stud cold-formed shear panels under monotonic and cyclic loading Part II: Numerical modelling and performance analysis", *Thin-Walled Structures*, Vol. 42, pp. 339–349, 2004.

15. Xu, L. and J. Martinez, "Strength and Stiffness Determination of Shear Wall Panels in Cold-Formed Steel Framing", *Thin-Walled Structures*, Vol. 44, pp. 1084–1095, 2006.

16. Corte, G. D., L. Fiorino and R. Landolfo, "Seismic Behavior of Sheathed Cold-Formed Structures: Numerical Study", *Journal of Structural Engineering*, Vol. 132, No:4, pp. 558–569, 2006.

17. Corte, G. D., L. Fiorino and R. Landolfo, "Seismic Behavior of Sheathed Cold-Formed Structures: Physical Tests", *Journal of Structural Engineering*, Vol. 132, No:4, pp. 570–581, 2006.

18. Dubina, D., "Behaviour and performance of cold-formed steel-framed houses under seismic action", *Journal of Constructional Steel Research*, Vol. 64, pp. 896–913, 2008.

19. Simsir, C. C. and A. Jain, "Nonlinear Analysis of Woodframe ShearWalls", *The 14th World Conference on Earthquake Engineering*, 2008, Beijing, China.

20. Fiorino, R., O. Iuorio and R. Landolfo, "Sheathed cold-formed steel housing: A seismic design procedure", *Thin-Walled Structures*, Vol. 47, pp. 919–930, 2009.

21. Landolfo, R., L. Fiorino and O. Iuorio, "A specific procedure for seismic design of cold-formed steel housing", *Advanced Steel Construction*, Vol. 6, pp. 603–618, 2010.

22. Schafer, B. W., Z. Li and C. D. Moen, "Computational modeling of cold-formed steel", *Thin-Walled Structures*, Vol. 48, pp. 752–762, 2010.

23. Fiorino, L., O. Iuorio and R. Landolfo, "Seismic analysis of sheathing-braced cold-formed steel structures", *Engineering Structures*, Vol. 34, pp. 538–547, 2012.

24. Peterman, K. D., N. Nakata and B. W. Schafer, "Hysteretic characterization of cold-formed steel stud-to-sheathing connections", *Journal of Construction Steel Research*, Vol. 101, pp. 254–264, 2014.

25. Peterman, K. D., N. Nakata and B. W. Schafer, "Sheathed Cold-Formed Steel Studs under Axial and Lateral Load", *Journal of Structural Engineering*, Vol. 140(10):04014074, 2014.

26. Asteris, P. G., L. Cavaleri, F. D. Trapani and V. Sarhosis, "A macro-modelling approach for the analyis of infilled frame structures considering the effects of openings and vertical loads", *Structure and Infrastructure Engineering*, pp. 551–566, 2015, `http://dx.doi.org/10.1080/15732479.2015.1030761`.

27. Karabulut, B. and S. Soyöz, "Experimental and analytical studies on different configurations of cold-formed steel structures", *Journal of Construction Steel Research*, Vol. 133, pp. 535–546, 2017.

28. Schafer, B. W. and M. ASCE, "Local, distortional, and Euler Buckling ıf Thin-walled Columns", *Journal of Structural Engineering*, Vol. 128, pp. 289–299, 2002.

29. Yu, W. W. and R. A. LaBoube, *Cold-Formed Steel Design*, John Wiley & Sons, Inc., New York, NY, USA, 2010.